Investigation of Variability in Skin Tissue Intrinsic Thermal Conductivity Measurements

by

Andy Tsai

B.S., Electrical Engineering
University of California, San Diego
(1993)

Submitted to the
DEPARTMENT OF ELECTRICAL ENGINEERING AND
COMPUTER SCIENCE
in partial fulfillment of the requirements

for the degree of

MASTER OF SCIENCE

at the

MASSACHUSETTS INSTITUTE OF TECHNOLOGY

May 1995

Signature of Author: _____
Department of Electrical Engineering and Computer Science
May 12, 1995

Certified by: _____ 5/16/95
H. F. Bowman
Director, MIT Hyperthermia Program
Senior Academic Administrator for the Harvard-MIT
Division of Health Science and Technology
Thesis Supervisor

Accepted by: _____
F. R. Morgenthaler
Chairman, Departmental Graduate Committee

Investigation of Variability in Skin Tissue Intrinsic Thermal Conductivity Measurements

by

Andy Tsai

Submitted to the Department of Electrical Engineering and Computer Science
on May 12, 1995 in partial fulfillment of the
requirements for the degree of

Master of Science

in Electrical Engineering and Computer Science

ABSTRACT

The Thermal Diffusion Probe 200 (TDP200) is a thermal properties characterization device that is capable of measuring the thermal conductivity of phantom materials with less than 0.2% variability. However, this device gives 1.5% to 2% variability in thermal conductivity values when the medium being measured is human skin tissue.

Six different sources of variability have been identified that might contribute this order of magnitude increase in measurement variability as the medium being measured is changed from phantom materials to skin tissue. The sources of variability include: the low sampling rate of the TDP200 system; baseline temperature fluctuations of the skin tissue; random perfusion effects of the blood vessels within the skin tissue; variable thermal contact between the measuring thermistor probe and the skin tissue; the dependence of thermal conductivity on the applied incremental heat temperature step; and inherent hydration induced skin tissue intrinsic thermal conductivity changes. Each of these possible sources of variability are carefully examined through simulations with Matlab, experiments both in-vitro and in-vivo, and theoretical calculations. The contribution from each of these variability sources are then quantified. This investigation is able to show that these six sources of variability account for the majority of the observed skin tissue intrinsic thermal conductivity measurement variability. On average, these variability sources combine to cause about 1.2% variability in the measurements.

Thesis Advisor: Dr. H. Frederick Bowman

Title: Director, MIT Hyperthermia Program
Senior Academic Administrator for the Harvard-MIT Division of Health Science and Technology

Acknowledgments

Many people directly and indirectly contributed to the work in this thesis. I would like to take this opportunity to thank them individually.

I wish to express my gratitude to my thesis advisor Dr. H. Frederick Bowman whose guidance and advice made possible the preparation of this thesis. I am sincerely grateful to Dr. William Newman from whom I have learned much in the course of this work. I like to give special thanks to the members of the research group, Dr. Gregory Martin, Dr. Ken Szajda, and Daniel Sidney for entertaining my questions and giving me the technical support that I needed. I am indebted to my friends for all the good times that I have had while studying at MIT. I also like to thank these friends for providing me with an atmosphere here that allowed me to keep what little sanity that I had left.

Dedications

I would like to dedicate this thesis to my family: my father Jason for always pushing me to do my best and believing that there isn't anything that I can't do; my mother Kerry for being my safety net, always supporting me and comforting me during my trying times; and my brother Billy for giving me the encouragement and the strength to strive toward my goals. This chance to credit them for what they have done for me is enough to justify the writing of this thesis.

Table of Contents

List of Tables

List of Figures

Chapter 1

Introduction

1.1 Objective of this Research

The overall aim of this research is to investigate and quantify the various factors that adversely affect the ability of the Thermal Diffusion Probe (TDP) to non-invasively measure skin tissue intrinsic thermal conductivity, a measure of the ability of the skin tissue to conduct heat under steady state conditions. Thermal Diffusion Probe is a thermal properties measuring instrument that has been shown to non-invasively measure the intrinsic thermal conductivity of static or phantom medium such as agar gel repeatedly to within 0.2% of its true value. It has also been shown that this 0.2% measurement error is the precision limit of the present measurement system. Repeated intrinsic conductivity measurements done on dynamic media such as on the surface of skin tissue typically yield 1.5% to 2% variability from measurement to measurement. Percent variability is calculated by taking the standard deviation of a set of experimental values and dividing it by the mean of those experimental values. Absolute values of skin tissue intrinsic thermal conductivity varies considerably from person to person. Perfused skin thermal conductivity also varies significantly with position as well as with time at a given position. Therefore, to examine the variability of repeated measurements of skin tissue intrinsic thermal conductivity requires careful measurement and analysis.

Six major factors have been identified that might contribute to the observed spread in the measured thermal conductivity. These factors include the low sampling rate

of the TDP instrumentation; baseline temperature fluctuations and spatial temperature gradient of the skin tissue; temporal fluctuations in perfusion within the skin tissue; dependence of intrinsic thermal conductivity value on the applied temperature step of the measuring heat thermistor; non-ideal and non-constant probe-tissue thermal contact during measurements; and inherent hydration induced skin tissue intrinsic thermal conductivity variations. Measurements were performed on various types of tissue, in-vitro and in-vivo, to simulate and better understand measurements on skin tissue. Measurements were also conducted on gels of known thermal properties. The purpose of these experiments was to isolate and to specifically address each of the six major sources of variability. Theoretical simulations on Matlab were also implemented to evaluate and quantify the impact on the observed variability from some of these variability factors. Based on the study, conclusions are drawn regarding which of these error sources contribute the most to the variability in thermal conductivity measurements. The second part of the thesis deals with different approaches to try to remedy these major causes of the variability. These proposed solutions were implemented to test their effectiveness in reducing the effects of the major sources of variability. Based on the performance of these proposed solutions, recommendations are made for incorporation in future generations of the TDP200 instrument. The ultimate goal is to have the Thermal Diffusion Probe be able to non-invasively measure intrinsic thermal conductivity of dynamic media (tissue) with the same degree of accuracy as those measurements done on static media or phantoms.

1.2 Motivation and Significance of this Research

Techniques are sought to improve the reproducibility and accuracy of skin tissue thermal conductivity measurements. These improved techniques can be analogously applied to improve the accuracy of any human tissue thermal conductivity measurements. Increasing the reproducibility and accuracy of tissue intrinsic thermal conductivity

measurements translates to more than a proportional increase in the accuracy of tissue perfusion. Both tissue intrinsic thermal conductivity and perfusion are derived from an experimentally determined value of effective thermal conductivity. An accurate measure of these tissue thermal properties leads to a deeper understanding of the heat-transfer mechanisms occurring in the tissue, and solutions to applications of the bioheat transfer equation can be implemented with higher accuracy and efficiency. The specific bioheat transfer application that motivated this research is hyperthermia.

Hyperthermia (elevated temperature) can be defined as the treatment of cancer by raising the malignant tissue temperature to 41 ^{o}C or higher. Localized heating of these malignant tissues is generally accomplished by the use of ultrasonic or electromagnetic radiation with ultrasound becoming the more popular of the two. The advantages of using ultrasound as the method of heat delivery include its ability to non-invasively apply heat to the treatment volume and to deliver heat to deep tumors via focussing where the geometric gain more than offsets the attenuation losses. One effect of elevating cancer tissue temperature in opposition to bodily controls is the accelerating of the cellular metabolic processes in the tumorous tissues which cause the tissue to increase its nutritional and oxygen requirements. These imposed requirements may not be fully met by the tumorous tissues due to deficient blood supply. As a result, the cells in the tumors can not reproduce, leading to the arrest of the tumor growth and ultimately shrinkage. In addition to causing direct irreversible damage to the diseased tissues, hyperthermia also indirectly enhances the effectiveness of other treatment regimes, notably X-radiation and chemotherapy. In recent years, advances in hyperthermia equipments and temperature monitoring capabilities has progressed considerably and has become a useful clinical modality for cancer therapy; however, it is still very short of perfection.

One of the major limitations of hyperthermia is the inability of the heat

applicator to preferentially heat and maintain the target tissue volume at the therapeutic temperature level for the required period of time. If the achieved temperature of the tumor deviates from the therapeutic temperature level just by a little, it can mean large differences in tumorous cell killing. At the same time during treatment, the temperature to the normal tissue surrounding the target volume must be kept low, below toxic levels. These normal surrounding tissues, though frequently not as sensitive to heat damage as tumorous tissues, are still very much affected by the heat dose. These are very tight treatment constraints that must be met by the hyperthermia clinician performing the treatment. Indeed, there is a crucial need to develop the capability to focus thermal energy on irregularly shaped target volumes while sparring surrounding tissue.

Achieving a therapeutic temperature level and restricting uniform temperature field within tumors is difficult due to the temperature field's dependence on both the tissue intrinsic thermal conductivity and the tissue blood flow. The intrinsic thermal conductivity of the tissue carries heat away from the tissue through conduction. With accurate knowledge of this value, the clinician can plan accordingly to adjust for that loss of applied heat. Blood flowing through a small tissue volume, known as perfusion, acts as a local heat sink. It cools the heated area through convection. Perfusion in tumors, as in normal tissues, is extremely heterogeneous in space and variable in time in an unpredictable manner. As a result, to obtain a steady heating temperature profile across the target tissue and low heat dose to normal surrounding tissues, perfusion rates at specific sites of the treatment area must be known both accurately and in real time. With this knowledge, the heat applied to the treatment area can be adjusted to compensate for changes in heat removal due to perfusion. Calculation of perfusion rates at a given point in tissue requires an accurate knowledge of the tissue intrinsic thermal conductivity of that point. The perfusion rate ω is calculated from the following equation:

$$\omega = \frac{\left(K_{eff} - K_m\right)^2}{K_m C_{bl} a^2} \tag{1.1}$$

where K_m = the tissue intrinsic thermal conductivity, K_{eff} = tissue effective thermal conductivity, C_{bl} = specific heat capacity of blood, and a = surface radius of the spherical thermistor bead. Small variability in measured value of K_m can greatly affect the accuracy of the derived value of ω [1]. This relationship can be obtained by taking the partial derivative of equation 1.1 with respect to K_m. The result is shown in equation 1.2.

$$\frac{\partial \omega}{\partial K_m} = -\left(\left(\frac{K_{eff} + K_m}{K_{eff} - K_m}\right) \cdot \frac{\omega}{K_m}\right) \tag{1.2}$$

Dividing the above result by ω/K_m transforms this equation into an equation relating percentage variabilities as shown in equation 1.3.

$$\frac{\frac{\partial \omega}{\partial K_m}}{\frac{\omega}{K_m}} = \frac{\partial \omega / \omega}{\partial K_m / K_m} = \frac{\%\text{var } \omega}{\%\text{var } K_m} = -\left(\frac{K_{eff} + K_m}{K_{eff} - K_m}\right) \tag{1.3}$$

To get the relative magnitude of the relationship between variability in tissue intrinsic thermal conductivity to variability in perfusion, assume that the percent variability associated with measured value of K_m is 1%, and calculate the percentage variability associated with perfusion as a result of that. Table 1.1 [2] summarizes the effect of this measurement variability on the precision of the derived value of perfusion ω in different tissues. As shown in the table, small variability of 1% in measured value of K_m translate to unacceptably large variability in perfusion. The lower the level of perfusion in the tissue, the bigger is the variability in the measured value of the tissue perfusion. This is because with low perfusion, K_{eff} is very close in value to K_m so the difference between K_{eff} and K_m

is small. When this difference is small, the quantity described in equation 1.3 is large. Thus for the same percentage variability in K_m, percent variability in perfusion is larger for tissue at lower perfusion. Spleen is a poorly perfused tissue thus it is much more adversely affected by variability in measured value of K_m. The perfusion level of the liver is higher than the perfusion level expected from the skin. But even with a high perfusion level, it is still showing over a 12% variability in measured value of perfusion due to a 1% variability in measured value of K_m.

Tissue	percent variability in K_m (%)	K_{eff} (mW/cm-^oC)	K_m (mW/cm-^oC)	ω (ml/100gm-min)	percent variability in ω (%)
Liver	1.00	5.48	4.68	80	-12.70
Prostate	1.00	5.63	5.16	47	-22.96
Spleen	1.00	5.50	5.38	11	-98.91

Table 1.1: Illustration of intrinsic thermal conductivity measurement variability leading to perfusion measurement variability

To further illustrate the idea of variability in K_m leading to large variability in ω, a parametric analysis of equation 1.3 was performed in Matlab. The result of the simulation is shown in Figure 1.1. The two parameters, perfusion ω and intrinsic thermal conductivity K_m, are varied over a reasonable range typical of surface skin tissue measurements. Notice in Figure 1.1 that as perfusion rate decreases, or as intrinsic thermal conductivity value increases, perfusion measurements become more and more sensitive to variations in K_m.

Depending on the measured intrinsic thermal conductivity and perfusion level of the skin, it is expected that a 1% variability in K_m of the skin will give rise to about a 20% variability in measured value of perfusion. Therefore, to reduce the percentage variability in perfusion to the range of a few percent, improvements must be made on the

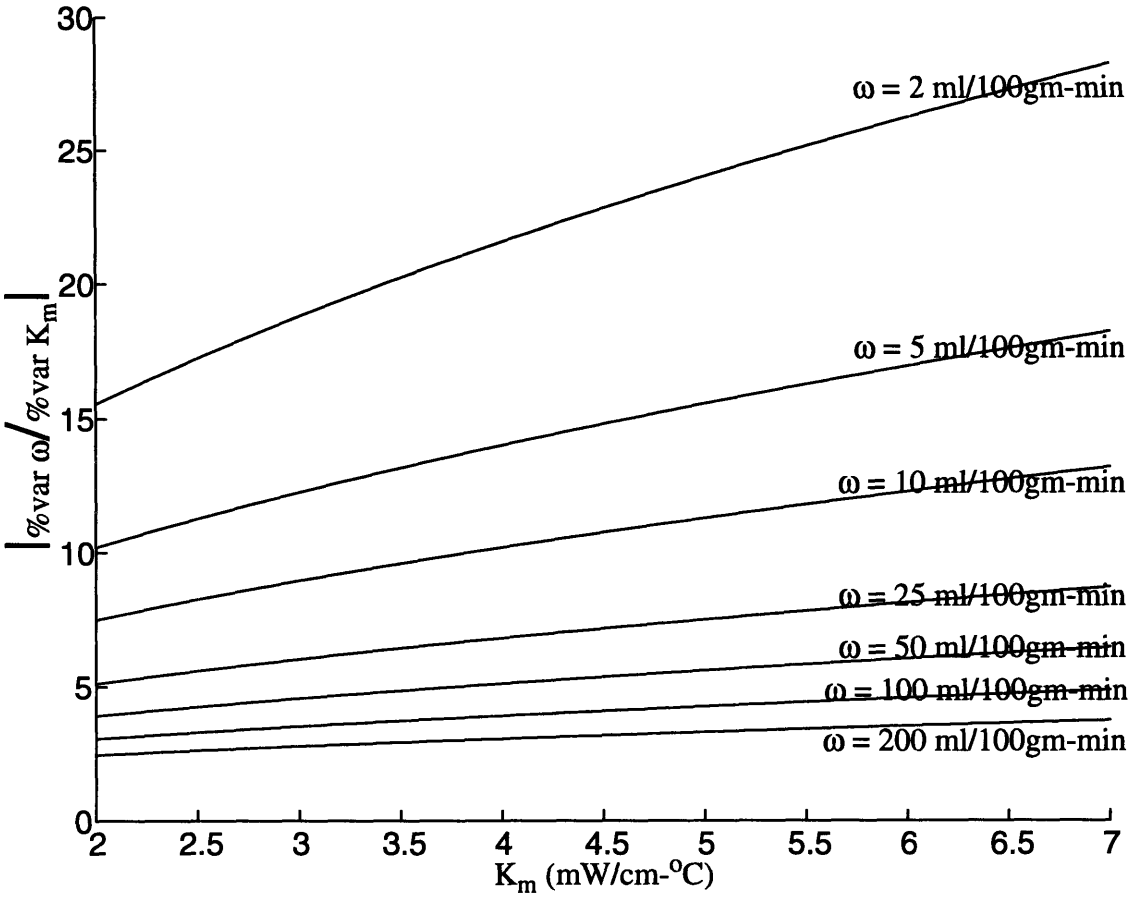

Figure 1.1. Variations in ω due to variations in K_m for different values of perfusion and intrinsic thermal conductivity.

measured accuracy of K_m, maybe to within a few tenth of a percent. This is the entire motivation behind this thesis, to try to reduce the variability in measured value of K_m so that perfusion ω can be measured more accurately.

Other important applications that can take advantage of this knowledge of thermal conductivity and perfusion include: thermography, electrocautery, laser angioplasty, laser arterial grafting, rf tissue oblation, etcetera [3]. The potential significance of this research may have dramatic impact on the ability to use skin perfusion characteristics to diagnose vascular diseases such as atherosclerosis. Perfusion levels can

be used to predict surgical outcomes in skin flap transfers, transplants, etcetera. If it can be shown that normal and tumor tissues have differing temporal characteristics, the extent of tumor might also be determined via perfusion measurements.

Chapter 2

Background

2.1 Nomenclature

A	=	heat flow cross sectional area (cm)
a	=	thermistor probe radius calibration constant (cm)
C_{bl}	=	specific heat of blood (W-sec/gm-^{o}C)
$f(t)$	=	transient power function (sec$^{-1/2}$)
h_o	=	zeroth order Steinhart-Hart calibration constant
h_1	=	first order Steinhart-Hart calibration constant
h_3	=	third order Steinhart-Hart calibration constant
K_b	=	thermistor probe thermal conductivity calibration constant (mW/cm-^{o}C)
K_{eff}	=	tissue effective thermal conductivity (mW/cm-^{o}C)
K_m	=	tissue intrinsic thermal conductivity (mW/cm-^{o}C)
$P(t)$	=	transient power response (mW)
P_{ss}	=	steady state power (mW)
R_{heat}	=	thermistor heat resistance (ohms)
R_{ladder}	=	TDP200 reference ladder resistance (ohms)
R_o	=	thermistor baseline resistance (ohms)
t	=	time (sec)
T_{heat}	=	heat temperature (^{o}C)

T_o = baseline temperature (^oC)

α_{eff} = tissue effective thermal diffusivity (cm^2/sec)

α_m = tissue intrinsic thermal diffusivity (cm^2/sec)

$\dot{q}_a'$ = ultrasonic applicator volumetric heat exchange (W/ml)

$\dot{q}_m'$ = metabolic volumetric heat exchange (W/ml)

ρc = volumetric heat capacity (W-sec/ml-^oC)

ΔT = volume average temperature step (^oC)

ω = tissue perfusion (ml/100gm-min)

%var K_m = percent variation in intrinsic thermal conductivity measurements (%)

%var $P_{ss}/\Delta T$ = percent variation of the ratio of steady state power to applied temperature increment measurements (%)

%var ΔT = percent variation in applied temperature increment measurements (%)

$\frac{\partial T}{\partial x}$ = temperature gradient in the direction of heat flow ($^oC/cm$)

2.2 Intrinsic Thermal Conductivity of Skin Tissue

There are several ways that heat can be transported in materials, namely by conduction, convection, or radiation. This thesis deals primarily with heat conduction through human skin tissue and is principally concerned with accurate reproducible measurement of intrinsic thermal conductivity of skin tissue. Intrinsic thermal conductivity, K_m, of skin tissue is defined as the quantity of heat, Q in milliwatts, transmitted in the direction normal to a unit surface area of skin tissue, in unit time, in steady-state conditions, and in response to a unit temperature gradient [4]. It is important to note that the associated heat transfer depends only on the temperature gradient created. Mathematically, this is described by Fourier Law of heat conduction as follows:

$$\frac{Q}{A} = -K_m \frac{\partial T}{\partial x} \quad . \tag{2.1}$$

Over the past, various individuals have measured the values of skin tissue intrinsic thermal conductivity using different methods. A short list of these values are compiled in Table 2.1 [4]. The skin tissue thermal conductivity values provided in Table 2.1 give use-

Finding	Tissue	Temp. (°C)	K_m (mW/cm-°C)	variability (%)	References
1	Skin, human	*in-vivo*	2.93 ± 0.16	5.46	Hensel & Bender 1956
2	Skin, human	37	2.66 ± 0.07	2.63	Bowman 1981
3	Skin, human, 1.6mm deep	37	4.98 ± 0.01	0.2	Bowman 1981

Table 2.1: List of reported skin tissue intrinsic thermal conductivity values

ful insights as to the range of values that can be expected for the measurements. It is interesting to note that finding number 3 is not measured from the surface of the skin but rather invasively into the skin tissue at a depth of 1.6 millimeters. Invasive measurements are not consistent with those performed in this thesis and hence cannot be used for comparison purposes.

2.3 Thermal Diffusion Probe

The Thermal Diffusion Probe (TDP200) Instrument System used in this study was provided by Thermal Technologies Inc. Chato in 1968 [5] first suggested the use of heated thermistor probe as a possible tool for measuring thermal conductivity. The Thermal Diffusion Probe technique was developed over the years by Bowman [1, 12], Balasubramaniam [6, 11], Valvano [3, 8, 10], and Newman [13]. A pulse decay approach

has been reported by Chen and Holmes [7]. The TDP200 is a micro-computer based instrument that is capable of non-invasively determining the thermal properties of perfused tissue, such as thermal conductivity, thermal diffusivity, and perfusion levels of skin tissue. The basis of how the TDP200 determines these characteristics lies in the self-heating capabilities of the electrically resistive thermistor bead mounted at the tip of a catheter probe and the heat transfer mechanisms of both the bead and the surrounding tissue.

The spherical thermistor bead of the TDP200 is normally configured to passively monitor the baseline temperature of the skin tissue. The way the TDP200 measures baseline temperature is by sending a small constant current (~0.1 mA) through the thermistor bead and measuring the voltage drop across the thermistor to determine its instantaneous resistance R. Once the resistant is obtained, it is mapped to temperature through the Steinhart-Hart equation:

$$T_o = \frac{1}{h_0 + h_1 ln(R) + h_3 (ln(R))^3} - 273.15 \quad . \tag{2.2}$$

Using this technique, the TDP200 can achieve temperature resolution of 0.004 ^oC.

After the baseline temperature T_o of the skin is established, the TDP200 reconfigures the bead as a heat source heating itself to an incremental temperature ΔT above the baseline temperature of the skin. The theoretical constant temperature to be achieved by the bead is $T_{heat} = T_o + \Delta T$. This is illustrated in Figure 2.1. To heat and maintain the thermistor bead at the heat temperature, the TDP200 first uses the Steinhart-Hart equation and works backwards to figure out the value of resistance that the thermistor needs to be set to in order to achieve the desired heat temperature in the bead. The instrument uses this resistance as the reference resistance and sets it as R_{ladder}. The TDP200 then drives the thermistor heat resistance R_{heat} to be equal to R_{ladder} with the use of an

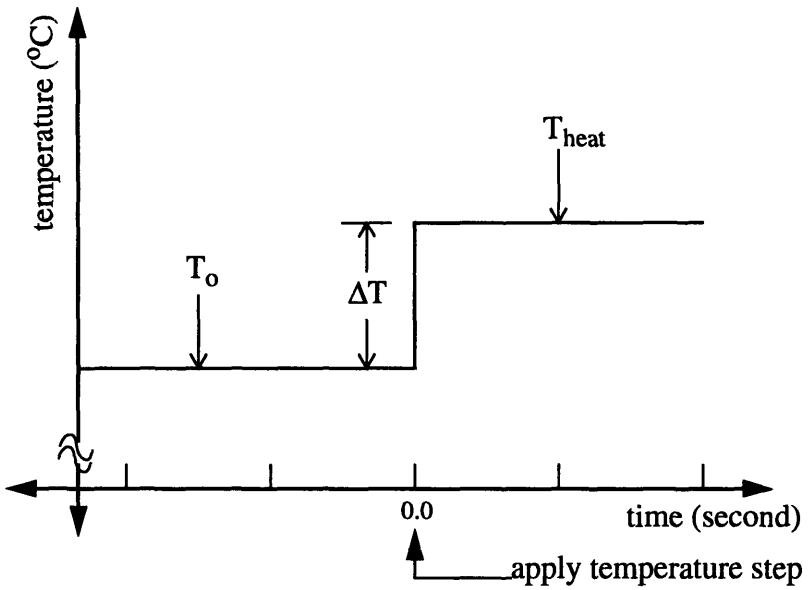

Figure 2.1. TDP200 thermistor bead temperature profile

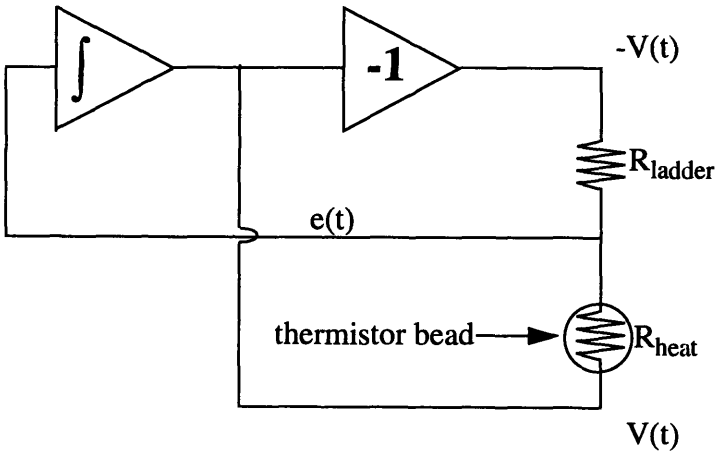

Figure 2.2. TDP200 electronic feedback circuit

electronic feedback circuit as shown in Figure 2.2. The circuit varies the input voltage V(t) so as to minimize the error voltage e(t) that is being fed back to the integrator. In essence, the feedback circuit stabilizes and fixes the error voltage e(t) at near zero volts making the voltage drop across both R_{heat} and R_{ladder} equal. The result is that with equal current and

equal voltage drop across the resistances, R_{heat} is held equal to R_{ladder}. The power response P(t) delivered to the bead in maintaining this constant temperature gradient while being surrounded by a conductive tissue medium is $V(t)^2/R_{ladder}$.

2.4 Application of Thermal Model in Measuring Thermal Conductivity

Heat transfer mechanisms in tissue include tissue conduction, metabolic heat generation, storage of thermal energy, convection due to blood flow, and energy absorption from external sources. Taking these five heat transfer mechanisms in a heat balance equation yields the following famous "bioheat equation" [9]:

$$\rho c \cdot \frac{\partial T}{\partial t} = \nabla\left(K_m \nabla T\right) - \omega c_{bl}\left(T - T_a\right) + \dot{q}_m{}' + \dot{q}_a{}' \,. \tag{2.3}$$

Valvano, Allen, and Bowman solved for the transient solution to the above bioheat equation for time-dependent, probe-tissue temperature response in the presence of perfusion [10]. The closed form solution provides the mapping from the power response P(t) of the TDP200 to the value of the intrinsic thermal conductivity K_m.

$$\frac{P(t)}{\Delta T} = \frac{4\pi a}{\dfrac{1}{K_m(1+\lambda a)} + \dfrac{1}{5K_b}}\left(1 + \frac{\dfrac{a}{\sqrt{\pi \alpha_m}}}{K_m\left(\dfrac{1+\lambda a}{K_m} + \dfrac{1-\lambda^2 a^2}{5K_b}\right)} f(t)\right) \tag{2.4}$$

where

$$f(t) = \frac{e^{-\lambda^2 \alpha_m t}}{\sqrt{t}} - \sqrt{\lambda^2 \alpha_m \pi}\, erfc\sqrt{\lambda^2 \alpha_m t} \tag{2.5}$$

and

$$\lambda^2 = \frac{\omega C_{bl}}{K_m} \tag{2.6}$$

In the absence of perfusion (ω=0) as in the case of static media or phantoms, the transient power function derived from the bioheat equation simplifies down to

$$\frac{P(t)}{\Delta T} = \frac{4\pi a}{\frac{1}{K_m} + \frac{1}{5K_b}} \left(1 + \frac{\frac{a}{\sqrt{\pi \alpha_m t}}}{1 + \frac{K_m}{5K_b}} \right) . \tag{2.7}$$

This is consistent with the thermal model formulated by Balasubramaniam and Bowman [11] for no blood flow. At infinite time ($t = \infty$) when the thermistor bead temperature has reached steady state, equation 2.7 reduces to

$$\frac{P_{ss}}{\Delta T} = \frac{4\pi a}{\frac{1}{K_m} + \frac{1}{5K_b}} . \tag{2.8}$$

By knowing the value of the steady state power P_{ss} applied to the bead, and the imposed temperature step, ΔT, the value of K_m can be derived. The way to obtain P_{ss} is by using least squares to fit a straight line to the plot of the power transient curve P(t) versus $t^{-1/2}$ and locating the y-intercept of the fitted line as P_{ss}. An example of the short time power transient response is shown in Figure 2.3 and the P(t) curve fit to $t^{-1/2}$ is shown in Figure 2.4.

Deriving K_m with the above method works very well in a static medium where the thermal conductivity is temporally invariant and perfusion ω is zero. TDP200 is able to reproducibly measure the intrinsic thermal conductivity of static medium repeatedly to within 0.2% of its true value. This is the precision limit of the present TDP200 system in the measurement K_m. This is shown to be the case in section 3.1 of this thesis. In a dynamic

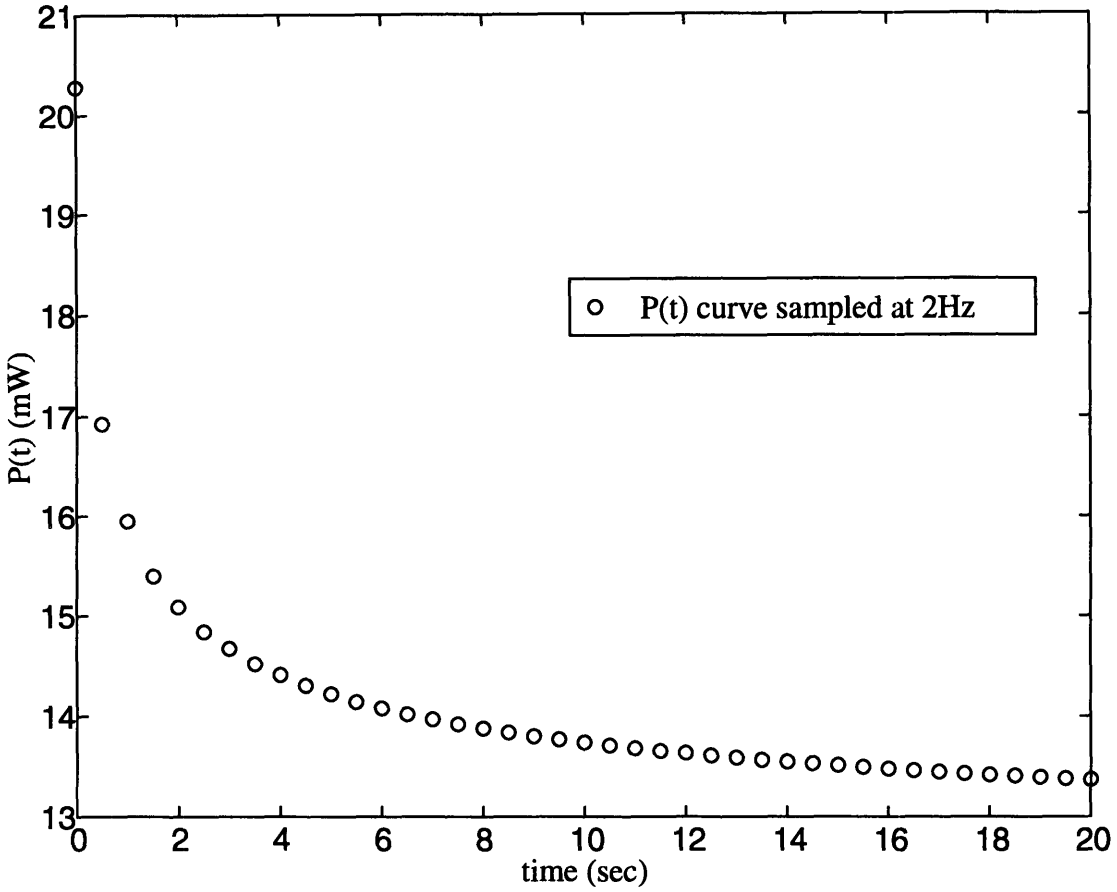

Figure 2.3. Sample of short time segment of power response P(t)

medium such as skin tissue, the simplification made earlier that perfusion is zero no longer holds true. Despite the fact, the TDP200 still uses the same approach in calculating the K_m for dynamic medium as in the static medium. The argument of using the same algorithm is based on the assumption that in a short transient time, the thermal field generated by the bead is not large enough to encompass much blood volume therefore the perfusion contribution is small. Hence, to a good approximation, perfusion effects are small and the simplification made earlier becomes valid again. That is, it is still valid to fit $t^{-1/2}$ to the short time transient power response and locating the y-intercept of the fitted line to arrive at the value of P_{ss} necessary for finding K_m.

Different short time windows of the power transient curve are available for the

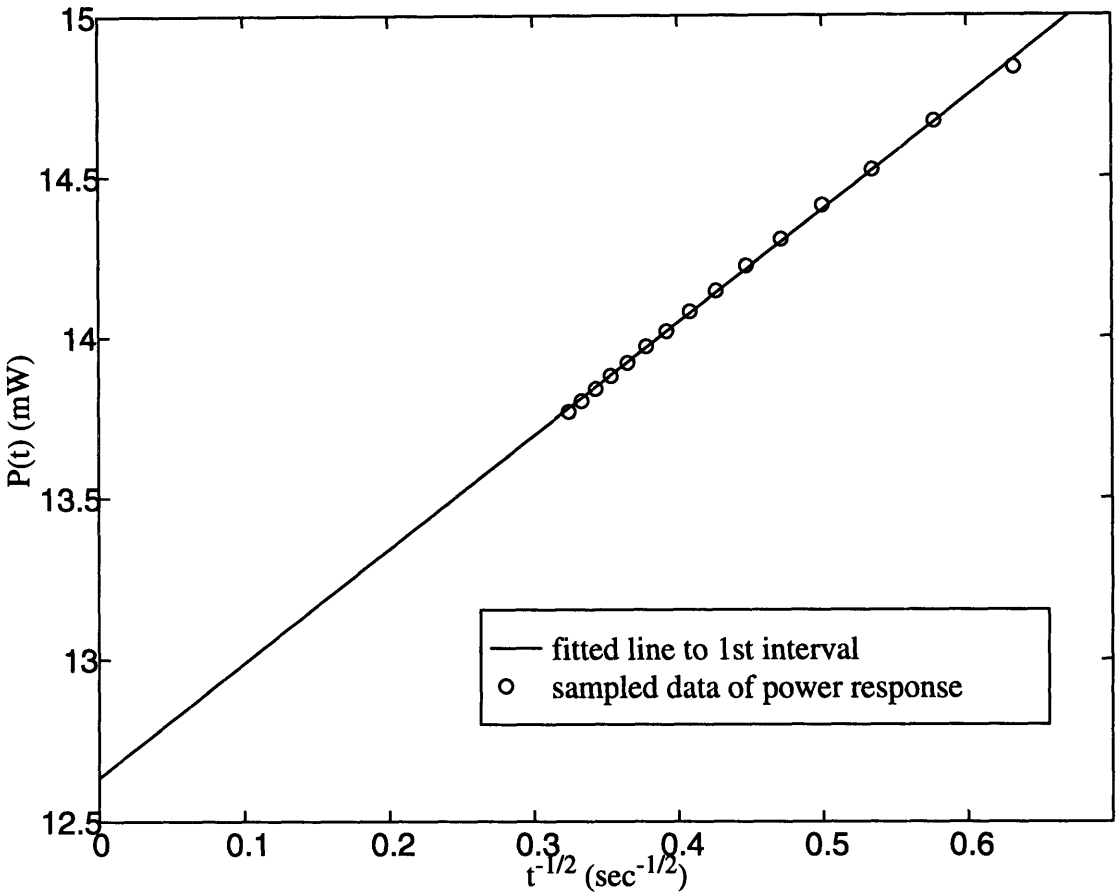

Figure 2.4. $t^{-1/2}$ fit to short time segment of P(t)

P(t) versus $t^{-1/2}$ fit. Table 2.2 lists the available fit intervals. The reason for picking the 2.5 second of the power response curve as the starting point of all these fit intervals is because that is approximately the amount of time it takes for the heat generated from the center of the bead to propagate to the surface of the bead where it is in contact with the skin tissue. One can think of the 2.5 seconds as the heating time constant of the bead. In general for static media, the different fit intervals give the same performance in terms of the derived K_m values. But interval 1 out performs fit intervals 2 through 5 when the medium is dynamic, therefore, it is used as the fit interval for the rest of this research. The reason that this interval works the best will become evident later in this thesis.

Interval Number	Starting Fit Time of P(t) (sec)	Ending Fit Time of P(t) (sec)
1	2.5	9.5
2	2.5	14.5
3	2.5	19.5
4	2.5	29.5
5	2.5	39.5

Table 2.2: TDP200 fit interval definition for determining P_{ss}

2.5 Modes of Operation

The TDP200 has two different modes of operation in making measurement of the power response curve: transient and continuous modes. In the transient mode, TDP200 samples P(t) of the heating thermistor bead at 2 Hz, which is the maximum sampling frequency of the present TDP200 system. In the continuous mode, the TDP200 only samples P(t) of the heating thermistor bead at 1 Hz. The sampling frequency is reduced by 50%. However, the advantage is that in the continuous mode, the TDP200 has the added feature of using a sense thermistor bead located approximately 1 centimeter away from the heat thermistor bead. With the sense thermistor bead located so close to the heat thermistor bead, it can track the baseline temperature variations of the skin tissue during heating. In this mode, the TDP200 alternates between sampling the temperature at the heat thermistor bead and the sense thermistor bead.

2.6 Surface Thermistor Probe

The existing thermistor transducer probes have all been designed and calibrated for the purposes of invasive tissue measurements where nearly the entire 4π surface area of the thermistor probe is exposed to the tissue medium during measurement. The use of these invasive probes for performing surface skin tissue measurements is not theoretically correct. In surface measurements, only about half of the surface of the thermistor bead is

exposed to the tissue medium. The probe is no longer exposed to the heat transfer capabilities of surrounding tissue with near 4π surface geometry but rather one with approximately 2π surface geometry. The calibration constants a_o and K_b calibrated for invasive measurements are not accurate for use in surface measurements. In addition, to maintain consistency of surface measurements in different experiments, the amount of the bead surface area exposed to tissue medium must be kept the same. To get around these problems, a surface thermistor probe is designed and fabricated based on the invasive thermistor probes. A sketch of the surface probe designed for skin tissue measurements is shown in Figure 2.5. The handle, or the cylinder rod of the surface mount probe, is made

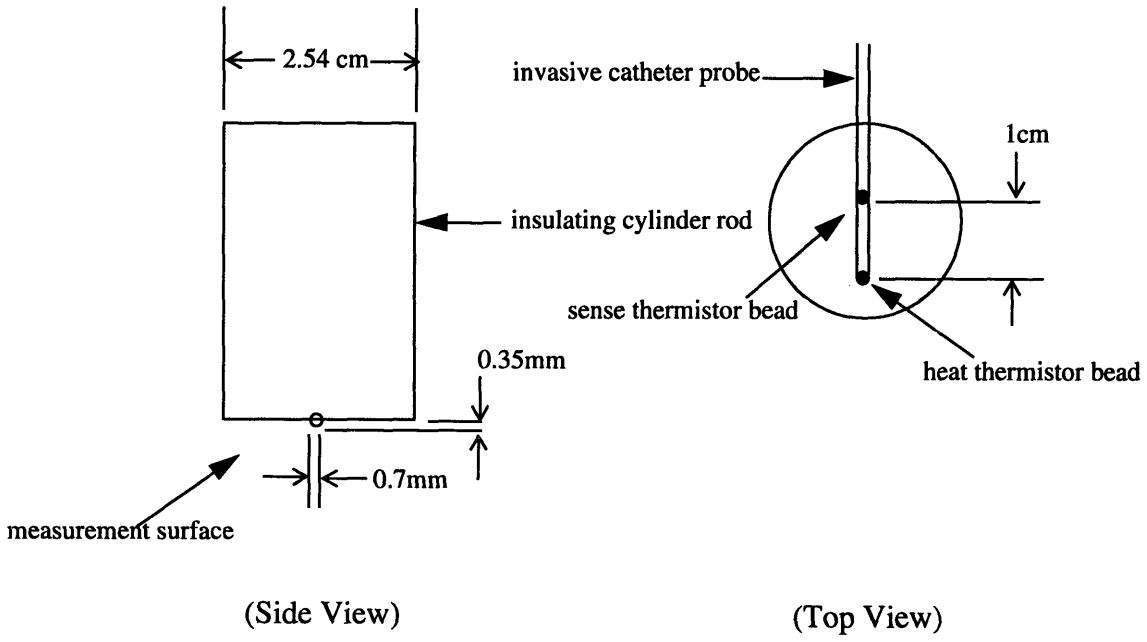

Figure 2.5. Surface thermistor probe

out of an insulating material called polyethylene. The rod is milled to a perfect cylinder and the end of the rod is squared and sanded to a smooth surface for better measurement

contact. A slit 2 centimeters long having a circular grove radius of the invasive probe, 0.35 millimeters, is machined in the cylinder rod end. The invasive probe is permanently attached into the grove allowing only half of the measuring surface of the thermistor probe to be exposed. With this surface probe, the amount of bead exposed to the tissue medium is always held constant. The two calibration constants of the surface probe, a_o and K_b, are calculated by placing the surface probe in 2 gel media of known but different thermal conductivity - agar gel with K_m = 6.23 mW/cm-^oC and glycerol mixture gel with 80% glycerol and 20% agar having K_m = 3.35 mW/cm-^oC. Based on the $P_{ss}/\Delta T$ values of the 2 gel media obtained from the surface probes, the calibration constants a_o and K_b are determined.

Chapter 3

Sources of Measurement Variability

The possible sources of TDP200 K_m measurement variability include the following:

- Instrument precision limit error. The inability to measure the exact temperature of the testing medium and the small number of acquired data points used for the linear regression to determine P_{ss} combine to cause variability in the measurements.
- Low sampling frequency. The 2 Hz sampling rate of the TDP200 system is thought to be too low to capture the high frequency components in the power response curve. By misrepresenting the true underlying power response data, it gives rise to variability in the measurements.
- Baseline temperature fluctuations. The assumption that the baseline temperature of the skin tissue is constant throughout the measurement period contributes to variability in the measurements.
- Random perfusion effects. The assumption that at the earliest times of the transient power response, perfusion is zero is not true. The zero perfusion assumption is based on the fact that at short times, the temperature field is only beginning to develop and thus the convection to conduction contribution to overall heat removal is small. Nevertheless, small fluctuations in perfusion can give rise to small changes in the instantaneous power requirements and thus to inaccuracies in extrapolated values of P_{ss}.

- Non-constant probe-tissue thermal contact. The non-ideal non-constant thermal contact made between the surface of the measuring probe and skin tissue introduces variations in the heat transfer.
- Dependence of K_m on ΔT. The applied temperature step ΔT in a set of measurements vary substantially because of the finite number of ladder settings. With K_m found to be a function of the applied temperature step, the derived value of K_m also varies due to varying ΔT.
- Inherent K_m variations. The variability observed may be due at least in part to natural changes in K_m as the level of skin hydration changes with time.

3.1 Instrument Precision Limit Error

Equation 2.8 can be rearranged to obtain the following equation:

$$K_m = \frac{1}{\frac{4\pi a}{P_{ss}/\Delta T} - \frac{1}{5K_b}} \quad . \tag{3.1}$$

As can be seen in this equation, the TDP200 uses the value of $P_{ss}/\Delta T$ to determine the value of K_m. Any errors occurring while measuring either P_{ss} or ΔT are cascaded and magnified over to errors in K_m. The TDP200 system is capable of measuring V(t) between 14 and 15 bits, or about 1 part in 20,000. With $P(t) = V(t)^2/R_{ladder}$, accurate measurement of V(t) translates to accurate measurement of P(t). Since P_{ss} is obtained by fitting P(t) to $t^{-1/2}$, the quantity P_{ss} can also be found very accurately. In essence, there is negligible variability associated with the derived quantity P_{ss} due to coarse resolution of the measuring system.

In contrast, there is a resolution limit associated with the measurement of temperature. The thermistor probe can measure temperature with a resolution of 0.004 °C. The 0.004 °C can be viewed as the quantization step of the measured temperature. Any temperature measurements taking on values not greater by 0.002 °C or not less than 0.002 °C from one another are considered as the same temperature. Each discrete temperature step represents a temperature measurement that span anywhere in the range ±0.002 °C of the discrete value. So, the real temperature can be thought of as a continuous random variable that is uniformly distributed in that range of ±0.002 °C of the discretized temperature. The standard deviation of this temperature random variable is $\sqrt{(0.002-(-0.002))^2/12} = 1.155\times10^{-3}$ °C. Assuming that the volume averaged imposed incremental temperature step ΔT is 6 °C, this means that ΔT can be measured with 0.0193% variability. This ΔT variability value is obtained by dividing the standard deviation of the temperature resolution by the measured temperature of 6 °C and multiplying by 100 to convert to percentages. In order to realize how much variability in K_m can be introduced by 0.0193% ΔT variability, a relationship between the two variabilities is found. Taking the partial derivation of equation 3.1 with respect to ΔT and dividing the result by $K_m/\Delta T$ yields the following relationship:

$$\frac{\%\text{var } K_m}{\%\text{var } \Delta T} = \frac{\partial K_m / K_m}{\partial \Delta T/\Delta T} = \frac{\frac{\partial K_m}{\partial \Delta T}}{\frac{K_m}{\Delta T}} = -\frac{4\pi a K_m}{P_{ss}/\Delta T}. \tag{3.2}$$

With %var ΔT = 0.0193% and using typical skin tissue surface measurement parameters of a = 0.13334 cm, K_m = 3.2464 mW/cm°C, $P_{ss}/\Delta T$ = 1.09 mW/°C, %var K_m is found to be -0.13%, or in absolute terms, just 0.13%.

The 0.13% variability in K_m measurements is the precision floor of the TDP200 system barring the effects of the TDP200's low sampling frequency. As can be

seen later in Figure 3.7, if the sampling frequency is much higher at beyond 50 Hz, the absolute precision limit of the TDP200 system is indeed 0.13%. It is due to the low sampling frequency of 2 Hz by the present TDP200 system that is degrading the precision limit of the system to 0.2% variability in K_m measurements. All in all, the 0.13% variability can be thought of as variability due to the coarse resolution of the temperature measurement. And the increase from 0.13% to 0.2% variability can be thought of as variability due to the low sampling rate of the TDP200 system.

3.2 Low Sampling Frequency

An accurate representation of the power response curve P(t) is critical in obtaining an accurate measure of skin tissue thermal properties. For skin tissue intrinsic thermal conductivity measurements, an accurate sampled version of P(t) is necessary to arrive at an accurate value for P_{ss}. An accurate measurement of P_{ss} is of the utmost importance because this value of P_{ss} is used in conjunction with equation 3.1 to arrive at the value of K_m. Any error associated with P_{ss} is magnified by over 6 times when the translation from P_{ss} to K_m is performed.

Presently, the TDP200 has the capability of sampling the power response curve P(t) at a maximum rate of 2 Hz. This amounts to being able to distinguish frequency components no higher then 1 Hz in the response curve P(t). With such a low sampling frequency, higher frequency components in P(t) are not being properly captured and might smear the sampled version of the power response curve. A corrupted sampled power response data P(t) is believed to be one of the causes for the large variations in skin tissue intrinsic thermal conductivity measurements.

The power response curve might contain high frequency components because of the effects of skin tissue perfusion. Blood flowing through the capillary network run-

ning underneath the skin surface, known as perfusion, plays a major part in thermal regulation of the body. Since P(t) is a measure of the heat regulation capabilities of the skin tissue, perfusion effects are heavily reflected in the power response curve. In other words, to a large extent, perfusion effects dictate the shape of the power response curve. For instance, when perfusion is increasing around the skin tissue being measured, the amount of heat being carried away by perfusion increases. To offset the amount of heat lost due to convection in the skin tissue, the amount of power supplied to the bead to maintain a fixed temperature step must increase. In essence, an increase in perfusion in the tissue leads to an increase in the power in the power response curve. With perfusion effects playing such a dominant role, their frequency characteristics are also likely to be reflected in the power response curve. Since tissue perfusion varies dramatically and in a very unpredictable manner, the power response curve will likewise do the same. If random perfusion of the tissue has frequency components higher then 1 Hz, which translates to a power response curve having frequency components greater then 1 Hz, the TDP200 is not going to be able to correctly represent those frequency components with a sampling frequency of 2 Hz. An illustration of such is shown in Figure 3.1. The aliasing effects due to low sampling rates might lead to errors in representing the power response curve P(t). The part of the power response curve that is the utmost importance to represent accurately is the first interval, or the 2.5th second to the 9.5th second, of P(t). This is because that is the part of the curve that is used in linear regression to determine P_{ss}.

To remedy the problem of low sampling rate, a peripheral data acquisition system as shown in Figure 3.2 was implemented to sample the power response curve at 1000 Hz. A large sampling rate of 1000 Hz is arbitrarily chosen to guarantee that the sampling frequency is more than sufficient to capture any frequency components that might be encountered. Prior to sending the raw analog voltage signal that represents P(t) to the

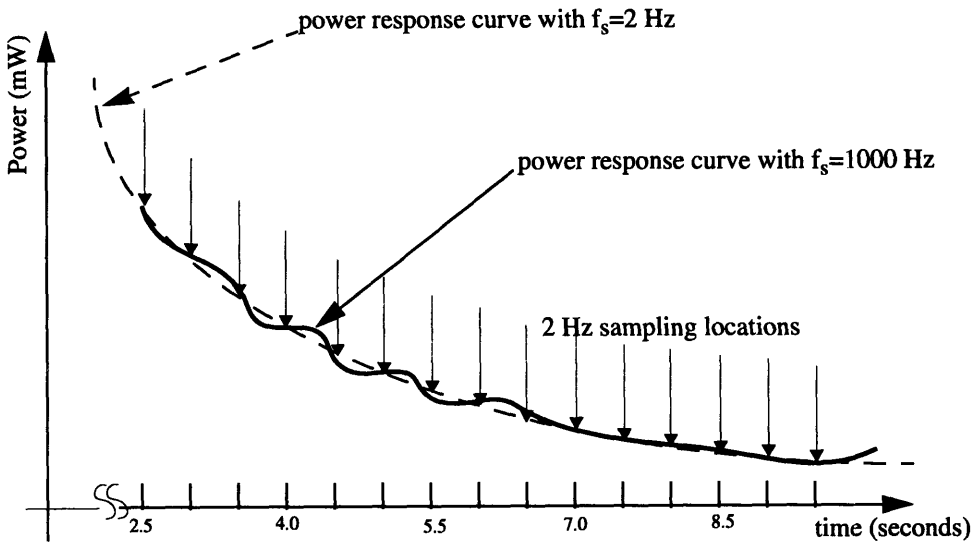

Figure 3.1. Low sampling rate of power response curve P(t)

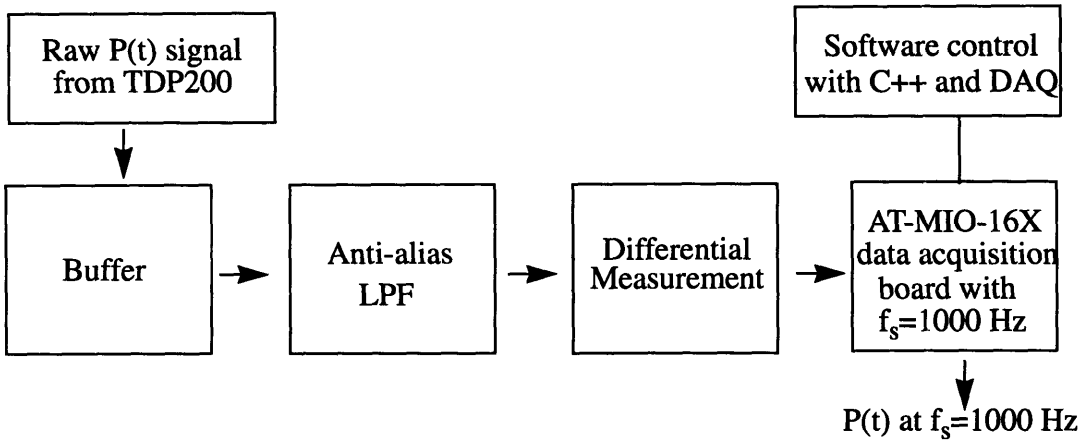

Figure 3.2. Peripheral data acquisition system setup

National Instrument AT-MIO-16X real time data acquisition board for sampling, the signal is first passed through a buffer and then to a second order active Sallen-Key low pass filter with a cutoff frequency of 500 Hz. This eliminates aliasing effects due to sampling.

The buffer and the low pass filter are all built with OP121 instrumentation op-amps to obtain the best noise rejection. To reduce the 60 Hz line and white noise pickup of the peripheral system, differential measurement mode data acquisition is used. With differential measurement, spurious noise sources cancel each other out and what is left is just the desired signal. To achieve differential measurement, the output from the low pass filter is connected to the positive differential input terminal of the acquisition board while the inverted output from the low pass filter is connected to the negative differential input terminal of the acquisition board. The circuit diagram of this setup is shown in Figure 3.3. The data acquisition software is written in Visual C++ and uses National Instrument Data

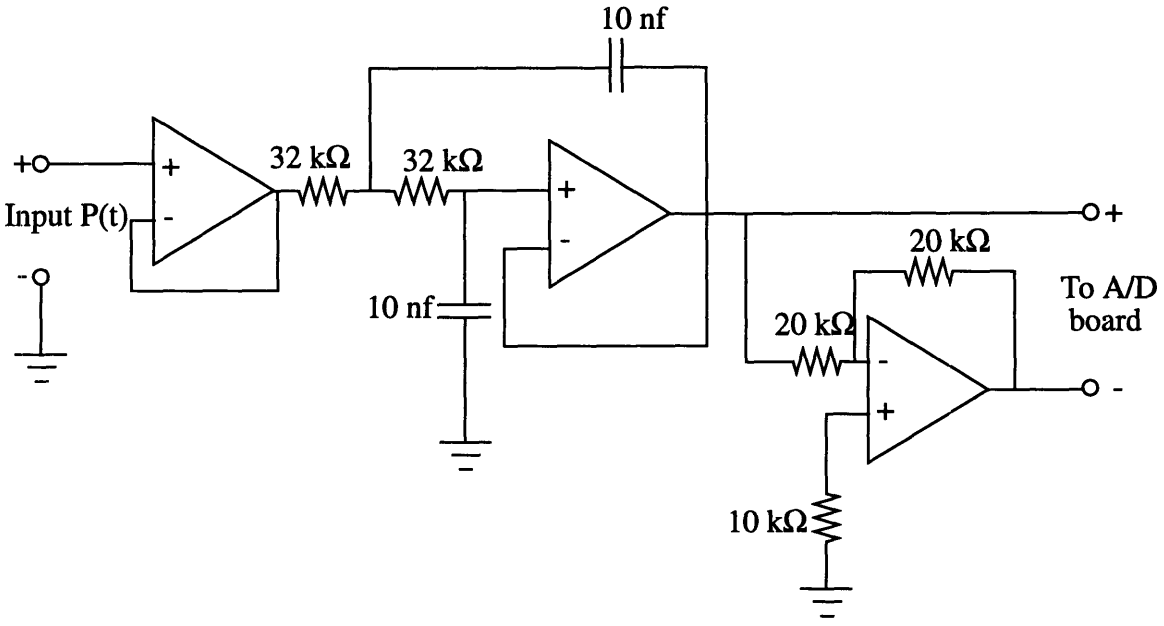

Figure 3.3. External circuitry for peripheral data acquisition system

Acquisition (NI-DAQ) supporting software for acquiring the sampled data. Circular data buffering is implemented to hold the acquired data. This type of data buffering allows the analog-to-digital acquisition board to acquire virtually infinite data samples in real time and is limited only by the amount of disk space available on the computer. The National

Instrument AT-MIO-16X board is a 16 bit analog-to-digital data acquisition board with input voltage ranging from -10 volts to 10 volts giving a voltage resolution of the output of 0.3 mV. An example of P(t)/ΔT obtained by sampling at 1000 Hz is shown in Figure 3.4. Notice in the figure that despite extreme care in shielding the system, using low noise components, and putting the system in differential mode of data acquisition, there are still traces of the 60 Hz noise riding on top of the true signal. However, the 60 Hz noise component is not large by any means when compared to the true underlying signal. Besides, the 60 Hz noise can be easily identified and notched out with a filter if deemed necessary. Calibration of the peripheral data acquisition system is done by adjusting the offset of the

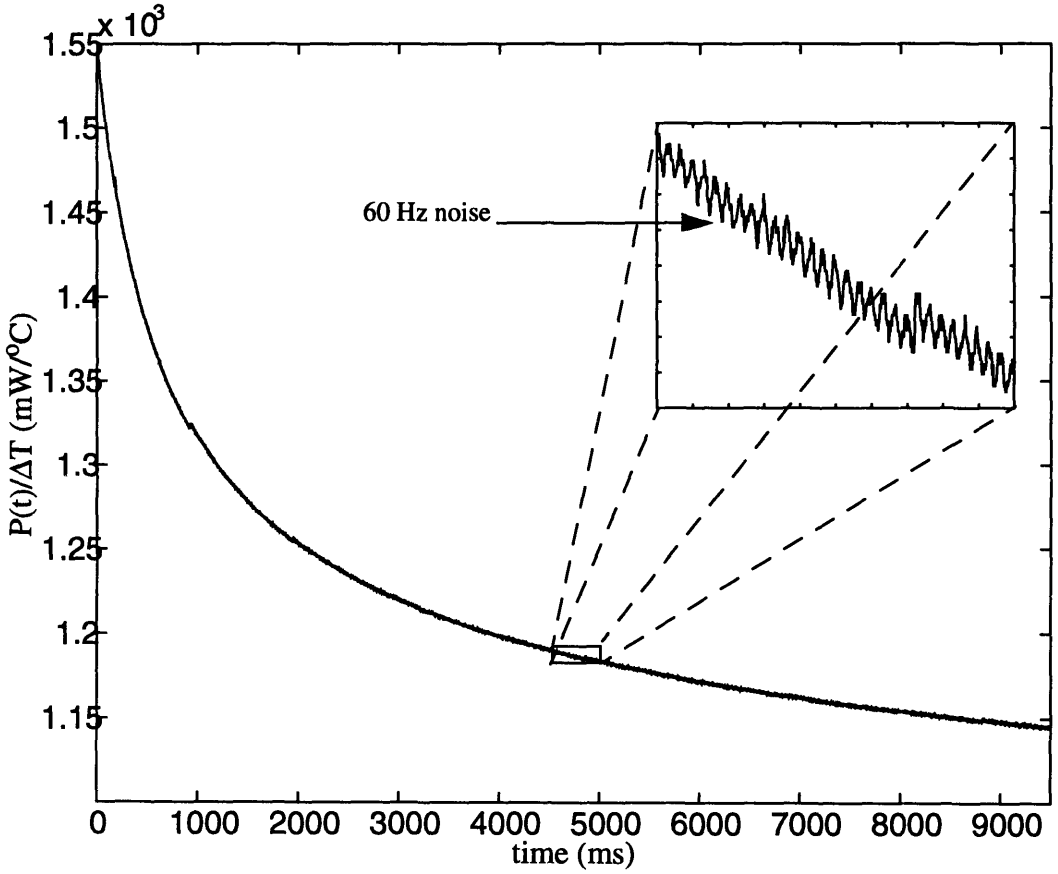

Figure 3.4. P(t)/ΔT measured on skin tissue with sampling frequency at 1000Hz

acquisition board. The offset of the acquisition board is adjusted until the peripheral data acquisition system can accurately match the 1 volt calibration reference voltage from the TDP200 to within one bit flicker, or 0.3 mV, of the true value.

To determine whether random fluctuations of perfusion are affecting the early times of the power response, frequency spectrums of experimental and theoretical P(t)/ΔT are compared against one another. If perfusion fluctuations are indeed corrupting the experimental P(t)/ΔT, then the frequency spectrum of the experimental P(t)/ΔT will show the existence of these corrupting perfusion frequencies while the frequency spectrum of the theoretical P(t)/ΔT will not. Peaks or humps will appear in the frequency response of the experimental P(t)/ΔT at the locations of the perfusion frequencies. A sample of the frequency spectrum of the experimental P(t)/ΔT data is shown on Figure 3.5. This figure is obtained by sampling P(t)/ΔT from measurements done on the skin tissue at 1000 Hz and taking the 7001-point Fast Fourier Transform (FFT) of the 2.5th second to the 9.5th second segment of P(t)/ΔT. The frequency spectrum of the theoretical P(t)/ΔT is shown on Figure 3.6. The theoretical P(t)/ΔT is obtained by fitting the same 2.5th second to the 9.5th second segment of the experimental P(t)/ΔT data to the equation $P(t)/\Delta T = \beta + \Gamma t^{-1/2}$. This is the equational form that P(t)/ΔT takes if perfusion ω is in fact zero. Based on equation 2.7, β and Γ are defined as follows.

$$\beta = \frac{4\pi a}{\frac{1}{K_m} + \frac{1}{5K_b}} \qquad \text{and} \qquad \Gamma = \frac{4\pi a}{\frac{1}{K_m} + \frac{1}{5K_b}} \cdot \frac{\frac{a}{\sqrt{\pi \alpha_m}}}{1 + \frac{K_m}{5K_b}} \tag{3.2}$$

The only difference between the theoretical and experimental P(t)/ΔT data is the effect of perfusion ω. Once β and Γ fit parameters are obtained from a least squares fit, a 7001-point FFT is likewise performed on the theoretical equation to arrive at the frequency spectrum. The 2.5th second to the 9.5th second time windowed segment of the curve is used in the

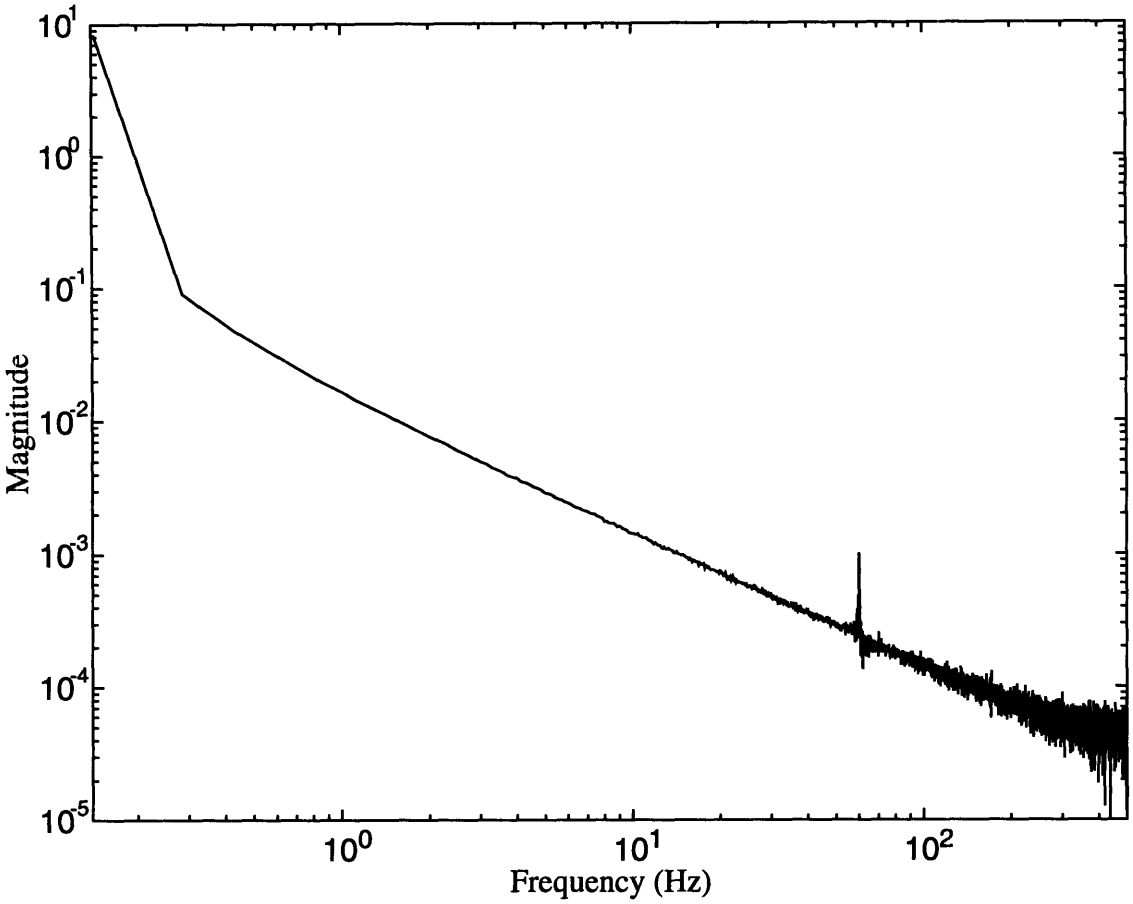

Figure 3.5. 7001-point FFT of experimental P(t)/ΔT

FFT because that is the fit interval and hence is of the greatest interest. The extrapolated value of P_{ss} is heavily dependent on these data points. A 7001-point FFT is picked for all the frequency spectrum calculations so that P(t)/ΔT data need not be zero padded during the frequency spectrum calculation. The advantage of not zero padding is that the resulting frequency spectrum calculated is very clean. The disadvantage of using such a small size FFT is that the frequency resolution of the spectrum is coarse. The spectrum can only distinguish frequency components 0.1428 Hz apart, but that is not too much of a concern. Knowing the exact frequency is not really an issue at this point. But what is important is

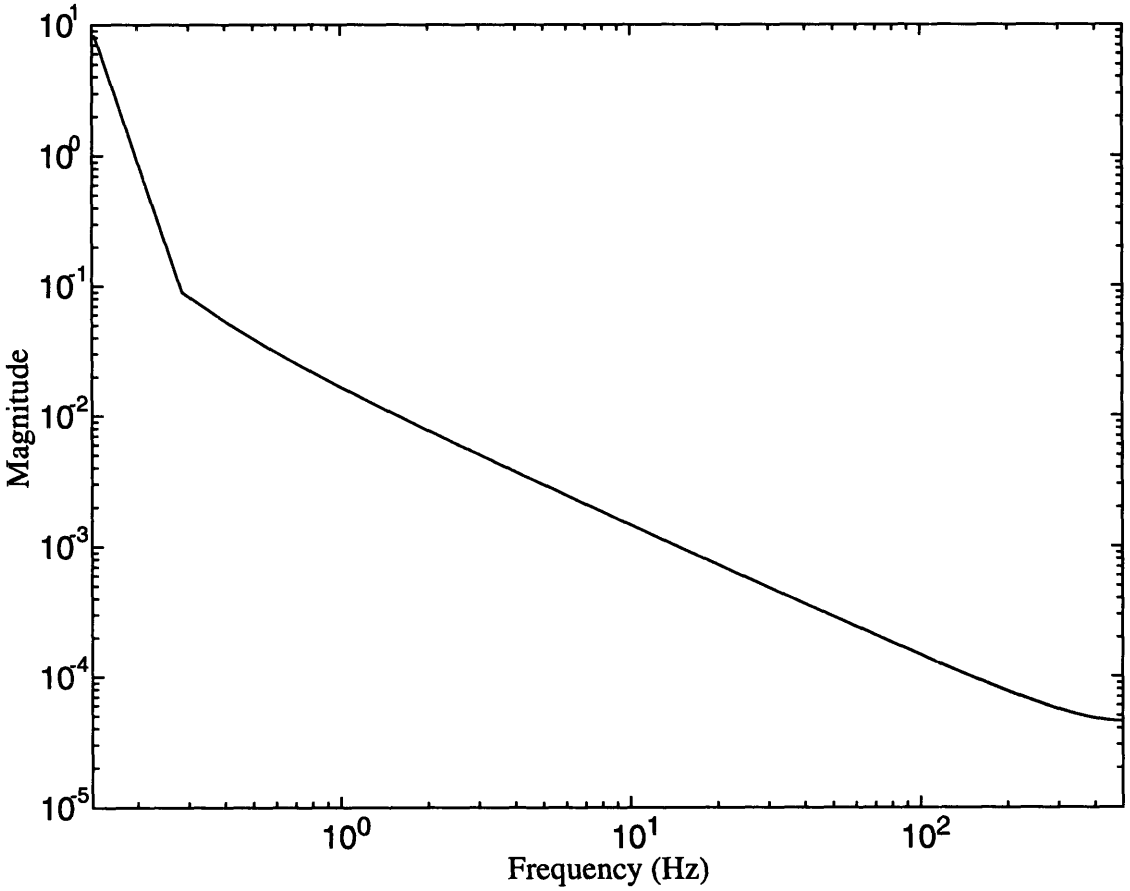

Figure 3.6. 7001-point FFT of theoretical P(t)/ΔT

being able to tell whether there exists perfusion frequency components above the Nyquist rate of 1 Hz or not.

While comparing between Figures 3.5 and 3.6, an observation can be made that the frequency spectrum of the two are almost identical with major differences between the theoretical and experimental data being the 60 Hz noise and the high frequency noise in the experimental data's frequency spectrum. The noise components are expected due to the non-ideal nature of experimental setup. The only thing that can be done with these noise components is to minimize their effects, which was accomplished in this case. The experimental data did not show any noticeable perfusion frequency compo-

nents in its frequency spectrum. Above the Nyquist rate of 1 Hz, there is definitely nothing of significance in the experimental frequency response. Thus it can be concluded that the random effects of perfusion are not corrupting the $P(t)/\Delta T$ data and that the 2 Hz sampling frequency of the present TDP200 is sufficient in representing all the signals present in $P(t)/\Delta T$ signal of the skin tissue.

With the capability of sampling the $P(t)/\Delta T$ increased to 1000 Hz, the question to ask next is whether the $P(t)/\Delta T$ data sampled at such a high frequency can improve the precision limit of the TDP200 system in measuring K_m. In the present TDP200 system where the sampling frequency is at 2 Hz, and when the first interval of the 2.5th second to the 9.5th second time window of the signal $P(t)/\Delta T$ is used, there are only 15 points that the TDP200 has at its disposal in its linear regression to find $P_{ss}/\Delta T$. With 1000Hz sampling frequency however, there can be as many as 7001 points used in the linear regression to find $P_{ss}/\Delta T$.

To investigate the effect of sampling on the precision limit of the TDP200, fifteen thermal conductivity measurements were performed on the surface of agar gels in a temperature controlled water bath with the $P(t)/\Delta T$ signal being sampled at 1000 Hz. The data from this set of fifteen measurements were continuously down sampled. In effect, down sampling is changing the sampling frequency of $P(t)/\Delta T$ for this set of fifteen measurements. Every time this set of data is down sampled to a new sampling frequency, a new set of K_m values is calculated. The variability of each new set of K_m values is also calculated. The result of this exercise is shown in Figure 3.7. With the sampling frequency increased up to 50 Hz, the precision floor of the TDP200 measuring system can be reduced down to around 0.13%. Sampling frequency higher than 50 Hz becomes counter productive in the sense that any further increase in sampling rate is not accompanied by any sizeable increase in the precision limit of the TPD200 in measuring K_m. The 0.13%

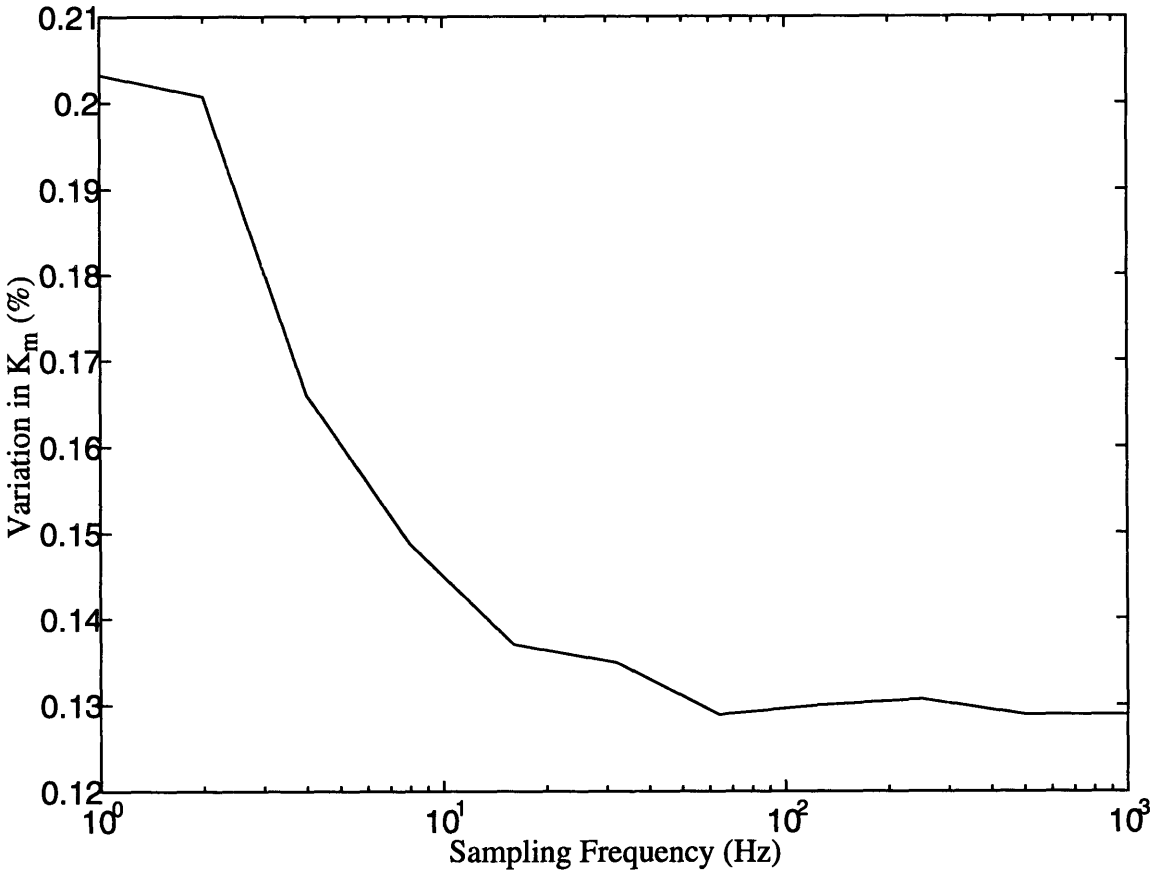

Figure 3.7. Effect of sampling on precision of TDP200 in measuring K_m

precision limit is consistent with the theoretically calculated value of the TDP200 precision limit done in section 3.1.

The speculation that the 2 Hz sampling frequency of the TDP200 is not high enough to capture the perfusion effects from the skin tissue is not true. As can be seen from the frequency spectrums, there are no perfusion forced frequency components above 1 Hz in $P(t)/\Delta T$ and hence the 2 Hz sampling of $P(t)/\Delta T$ is sufficient. In addition to resolving this speculation, higher sampling made it possible to show that by increasing the sampling frequency of the TDP200 to 50 Hz, it is possible to increase the precision limit of TDP200 in measuring K_m to about 0.13% variability.

3.3 Baseline Temperature Fluctuations

To obtain the intrinsic thermal conductivity of a medium, the value of $P_{ss}/\Delta T$ must be found experimentally. $P_{ss}/\Delta T$ is obtained by using least squares to fit a straight line to the plot of $P(t)/\Delta T$ versus $t^{-1/2}$ and extrapolating the straight line fit to infinite time in order to obtain the value of $P_{ss}/\Delta T$. Only the 2.5th second to the 9.5th second of the $P(t)/\Delta T$ data sequence is used for the straight line fit. At 2 Hz sampling frequency, that implies that the 6th to the 20th point of $P(t)/\Delta T$ are used. The power at each of the time points is obtained by squaring the voltage applied to the thermistor bead and dividing it by the bead thermistor resistance. ΔT is defined as the difference between the heat temperature T_{heat} and the baseline temperature T_o. Once the measurement begins, the thermistor bead configures itself as a heat source heating itself to a fixed temperature T_{heat} for the remaining part of the measurement. With the bead configured as a heat source, it can no longer be used to passively sense the baseline temperature T_o, and without that value, ΔT can not be known exactly. TDP200 gets around this problem by using the baseline temperature of the medium immediately prior to the experiment as the baseline temperature T_o and assumes that this value stays constant throughout the rest of the 10 second measurement. Essentially, TDP200 samples the baseline temperature of the medium prior to time zero and uses that value throughout the entire K_m measurement.

The question is whether using the baseline temperature of the medium immediately prior to measurement is a good approximation to use as the T_o for the rest of the measurement process. When thermal conductivity measurements are performed on static media such as agar gels, the media are placed in a water bath to ensure that their baseline temperatures do not vary from the set temperature of 37.3 ^oC. Extensive studies showed that in any 10 second windowed segment of the testing medium's temperature profile, the fluctuation is less then the temperature resolution of the thermistor bead of 0.004^oC. As a

result, baseline temperature fluctuation of a medium in water bath is concluded to be zero. So, in the case of static media, baseline temperature measured immediately prior to the experiment is an excellent approximation for T_o.

However, when measurements are performed on dynamic media such as on the skin tissue, the baseline temperature of the skin tissue fluctuates wildly and in an unpredictable fashion depending heavily on various factors such as the room temperature, the mood of the individual, and the location of the skin tissue where the measurements are performed. As a result, baseline temperature measured prior to measurement is no longer a good approximation of T_o during the measurement. Figure 3.8 illustrates this phenomenon.

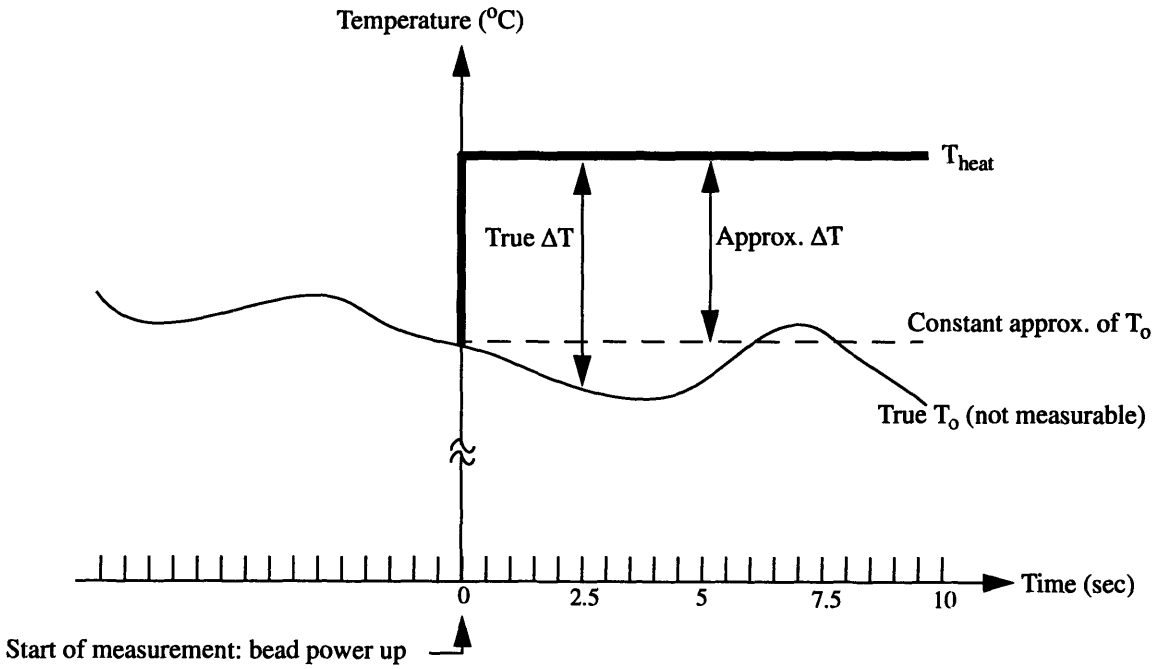

Figure 3.8. Illustration of baseline temperature fluctuations

The question is how large is the impact of this coarse approximation of T_o on K_m measurements. Before being able to answer this question, a measure of how much the

skin tissue temperature varies over a time window of 10 seconds needs to be known. A 10 second time window is chosen for the study because when interval one is used as the fit interval, that is the time duration in which the TDP200 approximates the baseline temperature T_o as being constant. Since skin temperature varies in a very random fashion and for lack of a better model, it is assumed that skin temperature is a normally distributed random variable with a mean and a standard deviation. The standard deviation of the skin temperature in that 10 second window gives a measure of the variability and helps answer just how bad is the TDP200's approximation to skin temperature being constant over a 10 second time window. Eight hundred 10 second time frame skin temperatures measurements were collected to estimate the standard deviation of the skin temperature to within 5% of the real value with a 95% confidence level. The mean value of this eight hundred sets of measurements is just the average of all the temperatures. The results of the study show that skin temperature has a standard deviation of 0.0047°C about its mean.

After knowing the amount of skin temperature variation, the next step is to examine the impact of this baseline temperature variation on K_m measurements. Variations in skin baseline temperature directly contributes to errors in ΔT since $\Delta T = T_{heat} - T_o$. The relationship between ΔT and T_o is one to one so T_o variations of 0.0047°C directly translates to ΔT variations of 0.0047°C. The negative sign is not taken into account since variability is sign insensitive. In a conventional measurement where ΔT is at 6 °C, the percent variation of ΔT comes out to be 0.0783%. A relationship needs to be obtained that can translate this error in ΔT to errors in K_m. Taking the partial derivative of equation 3.1 with respect to ΔT gets the following relationship:

$$\frac{\partial K_m}{\partial \Delta T} = -K_m^2 \cdot \frac{4\pi a}{P_{ss}} \quad . \tag{3.5}$$

Dividing the above result by $K_m/\Delta T$ and rearranging yields the following desired equation:

$$\frac{\frac{\partial K_m}{\partial \Delta T}}{\frac{K_m}{\Delta T}} = \frac{\frac{\partial K_m}{K_m}}{\frac{\partial \Delta T}{\Delta T}} = \frac{\%\text{var } K_m}{\%\text{var } \Delta T} = \frac{-4\pi a}{P_{ss}/\Delta T} \cdot K_m \quad . \tag{3.6}$$

With %var ΔT = 0.0783% and using typical measurement parameters of a = 0.13334 cm, K_m = 3.2464 mW/cm-°C, and $P_{ss}/\Delta T$ = 1.09 mW/°C, %var K_m is found to be -0.504%, or in absolute terms 0.504%.

To verify the above calculated results, a simulated experiment is conducted. For the experiment, fifteen sets of raw TDP200 data file is obtained. Each raw data file represents a thermal conductivity measurement of glycerol gel mixture composed of 80% glycerol and 20% agar. This composition of gel mixture is used because its thermal conductivity is close to that of skin tissue, 3.35 mW/cm-°C. The glycerol gel mixture is immersed in a water bath to guarantee baseline temperature stability during experimentation. The fifteen runs of this particular gel mixture K_m measurements give a 0.19% variability. This is basically the precision error source of the TDP200 measuring system. Therefore, it can be deduced that the fifteen sets of K_m measurement data is not being corrupted or influenced by other outside sources of error. To investigate the effects of baseline temperature variation, the fifteen sets of the glycerol gel mixture data is contaminated with baseline temperature variations. The contaminating baseline temperature variations are simply the temperature measurements made on the skin tissue. The fifteen sets of skin temperature measurements are obtained and superimposed onto those fifteen sets of raw data collected by the TDP200 while performing K_m measurements on the gel mixture. The way to superimpose the skin baseline temperature variations to raw gel mixture measurement data files is by reflecting the fifteen skin temperature baseline variations to variations

in ΔT of the fifteen individual measurement runs. The reason that this is justified is because $\Delta T = T_{heat} - T_o$ and variations in baseline temperature T_o is simply the negative of the variations in ΔT. The sign of the variation is irrelevant so it is ignored.

Based on the fifteen sets of data that are purposely corrupted by baseline temperature variations, K_m values are recalculated. The newly calculated K_m values show a variability of 0.50%. This increase in variability from 0.19% to 0.50% in K_m measurements is solely due to the effect of the baseline temperature fluctuations that are artificially introduced to the raw data files. Hasty assumptions might be made that the precision error of the measuring system and the error source due to the baseline temperature fluctuations are considered as synergistic or dependent sources of error. If that is true, then it can be inferred that the percentage error associated with baseline temperature fluctuations is 0.31%. This quantity is obtained simply by subtracting the system precision error of 0.19% from the final resulting percentage variation of 0.50%. However, it is much more accurate to assume that the TDP200 precision error source and the baseline temperature fluctuation error source are independent sources of error. There is really no connection between the two types of errors. In this case, the error contribution due to baseline temperature fluctuations would be 0.46%. This quantity is obtained by taking the square root of the difference in the square of the final resulting percentage variation of 0.5% and the square of the TDP200 precision error of 0.19% ($\sqrt{(0.50\%)^2 - (0.19\%)^2} = 0.46\%$). The 0.46% error is close enough to the estimated value of 0.50% to verify that the baseline temperature fluctuations give rise to approximately 0.50% error in the derived value of K_m.

TDP200 has the added feature of a sense thermistor bead located 1 centimeter away from the heat thermistor bead. The purpose of the sense bead is to help keep track of baseline temperature variations at the heat bead location. The reason that this can be done

is because the sense thermistor bead is located so close to the heat thermistor bead that it can give a very good first order approximation to baseline temperature variations around the heat bead. Eight hundred 10 second skin temperature measurements are performed again, but this time, the sense thermistor bead is used to help track the baseline temperature fluctuations. With the sense bead, the variability in baseline temperature is reduced down to 0.0037°C. Using equation 3.4 again, 0.0037°C variability in baseline temperature translates to 0.4% variability in measured value of K_m. This is an improvement of 0.1% in variability. However, the down side of using the sense bead is that the sampling frequency of the power response curve is reduced down from 2 Hz to 1 Hz. This reduction in sampling frequency increases the K_m measurement variability slightly as shown in Figure 3.7. After taking that into account, the improvement in variability from using a sense bead to track baseline temperature fluctuations is reduced. The improvement in K_m measurements using a sense bead is too small to be meaningful. Thus it can be concluded that regardless of using sense bead or not, the baseline temperature fluctuation is still going to force about 0.5% variability in K_m measurements.

3.4 Random Perfusion Effects

Perfusion can be defined as the rate at which the quantity of blood in a given mass or volume of tissue is replenished at the level of the capillary network [12]. Perfusion is important to the skin because it plays a very pivotal role in the skin's heat regulation and also the skin's supply of oxygen and nutrient. Perfusion of the skin is a function of blood pressure and resistance. The blood pressure of humans changes quite dramatically depending on the state and mood of the individual. For example, high blood pressure might be linked to tension and nervousness. The flow resistance is mainly due to the dimensions of the vascular tree and arteriolar narrowing. These openings change in a very unpredictable manner depending on the position and functional need of the skin. For

instance, in response to cold weather, the dimensions of the skin tissue vasculatures contract and reduce in size to conserve heat. As a result, the unpredictable nature of blood pressure and resistance directly leads to unpredictability in skin tissue perfusion.

The thermal field generated by TDP200 to measure thermal conductivity interrogates a volume of skin tissue between 2 and 3 millimeters in diameter. This volume includes hundreds of capillaries and arterioles, hence it is safe to assume that fluctuations in the heat removal by blood flowing through them may impact the results of thermal conductivity measurements. To conceptualize this effect, imagine taking thermal conductivity measurements around a highly perfused skin tissue. The greater the perfusion level, the greater the heat removed by the skin. As a result, higher power must be given to the thermistor bead to maintain the same fixed incremental temperature step above baseline. In effect, perfusion alters the power response which leads to measured value of effective skin thermal conductivity which is then partitioned into an intrinsic thermal conductivity and a perfusion term. Since perfusion of skin appears to vary in a random manner, its influence on extracted values of intrinsic thermal conductivity will vary in a random fashion as well.

To get around the effect of perfusion fluctuations, the TDP200 fits only the early short time transient segment of the power response curve to $t^{-1/2}$ in order to extrapolate to the value of P_{ss}. This method employed by the TDP200 to reduce the effects of perfusion is based on the observation that in the very early time of the power response curve, the thermal field generated by the thermistor bead is very small thus interrogating a very small skin volume. Smaller skin volume means that it encompasses a smaller number of blood carrying vessels. A reduced number of blood vessels translates to smaller perfusion effects [13]. Based on this argument, interval one is chosen as the interval of fit since this interval is the shortest and hence the thermal field generated is the smallest as compared to the other longer time fit intervals. Although perfusion effects are reduced, they are still not

strictly speaking zero. As one might recall, fitting the power response curve to $t^{-1/2}$ to arrive at P_{ss} is only valid for the case when perfusion is truly zero. So regardless of how small perfusion effects have been reduced, they are still not zero, which means that it is not entirely correct to fit the power response curve to $t^{-1/2}$. This inappropriate use leads to measurement errors and is one of the major speculative causes of why skin tissue intrinsic thermal conductivity can not be measured very accurately.

The first step in this part of the investigation is to use computer simulations to observe and roughly quantify the effects of perfusion. Equation 2.4, the closed form solution to the bioheat equation, is implemented in Matlab for simulation. Though equation 2.4 used for the simulation might not perfectly describe the effects of perfusion, it is the best model that is available. Typical surface skin tissue measurement values are used for the equation parameters: a = 0.13334 cm, C_{bl} = 3.84 W-sec/gm-^{o}C [4], K_m = 3.2464 mW/cm-^{o}C, K_b = 0.1617 mW/cm-^{o}C, α_m = 0.32 cm^2/sec, and ΔT = 6 ^{o}C. To highlight the effects of perfusion, five P(t)/ΔT responses are generated with the curves taking on perfusion levels of ω = 0, 15, 30, 45, 60 ml/100gm-min. The selected range of perfusion levels is representative of the entire gamut of perfusion levels occurring in the early transient of the power response. The results of the simulation are shown on Figure 3.9. Notice in the figure that as the response progresses in time, the greater the perfusion, the greater the P(t)/ΔT versus $t^{-1/2}$ curve tend to show a curvature in the upward direction. The higher the perfusion, the more the curve diverges from a straight line. This upward curving shape is reasonable because with increasing time, the thermal field generated by the bead increases thus interrogating more and more blood vessels and the greater the fraction of total heat transfer that is due to perfusion. To keep up with the loss of heat due to perfusion, more power must be dumped into the bead. This increase in power is what gives rise to this upward trend in the P(t)/ΔT versus $t^{-1/2}$ curve. The zero perfused P(t)/ΔT versus $t^{-1/2}$ curve

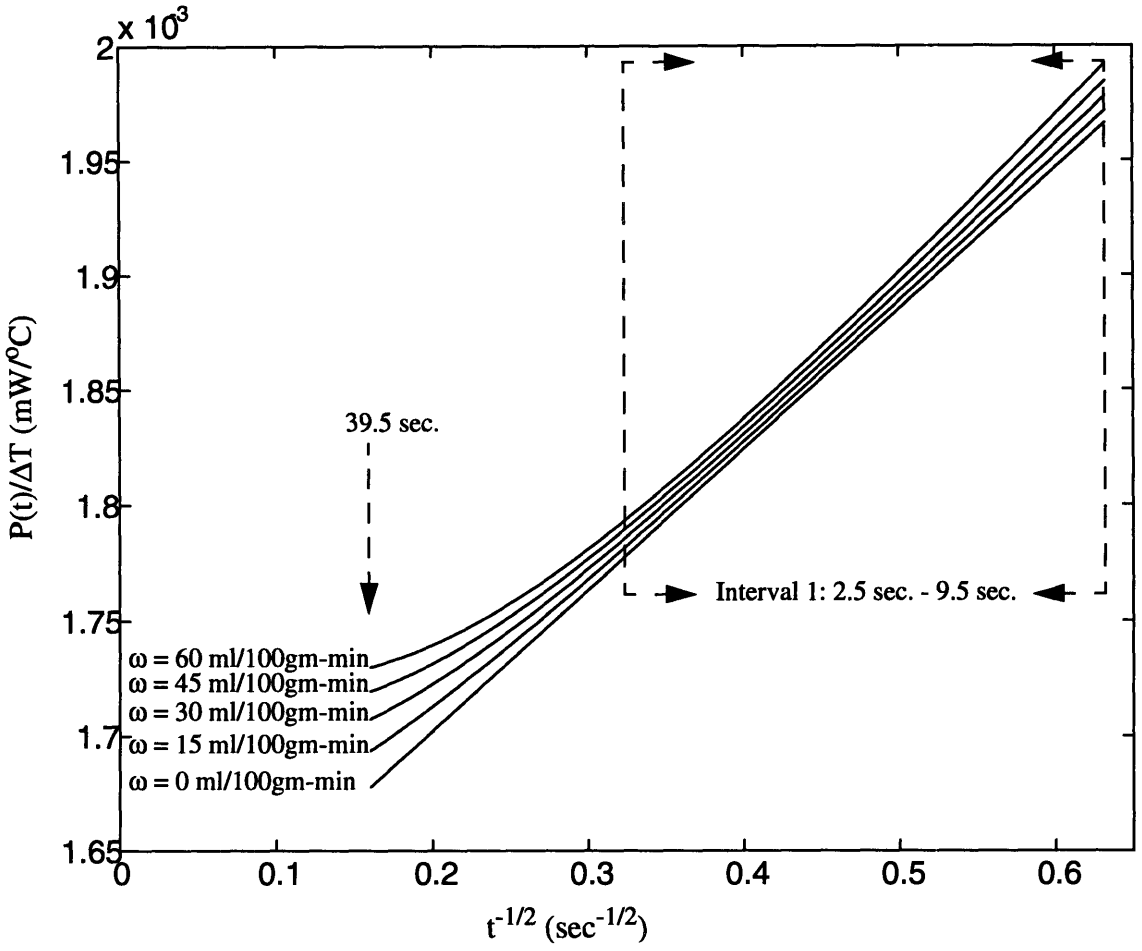

Figure 3.9. P(t)/ΔT with different levels of perfusion

continue to progress in a downward straight line manner as time progresses. By the time the five P(t)/ΔT curves reach the 39.5th second, the difference in values between the five curves is quite large. It is this large difference that affects the straight line fit of P(t)/ΔT to $t^{-1/2}$. As a result, the straight line extrapolated $P_{ss}/\Delta T$ values from the five curves are going to be substantially different, meaning that the derived value of K_ms are going to different as well. However, as can be observed in Figure 3.9, if the straight line fit is performed using the first interval, the effects of perfusion have not come into play thus perfusion effects are avoided. Figure 3.10 shows the straight line fit of $t^{-1/2}$ to the five P(t)/ΔT curves and the resulting $P_{ss}/\Delta T$ values when interval one is used as the fit interval. Notice that the

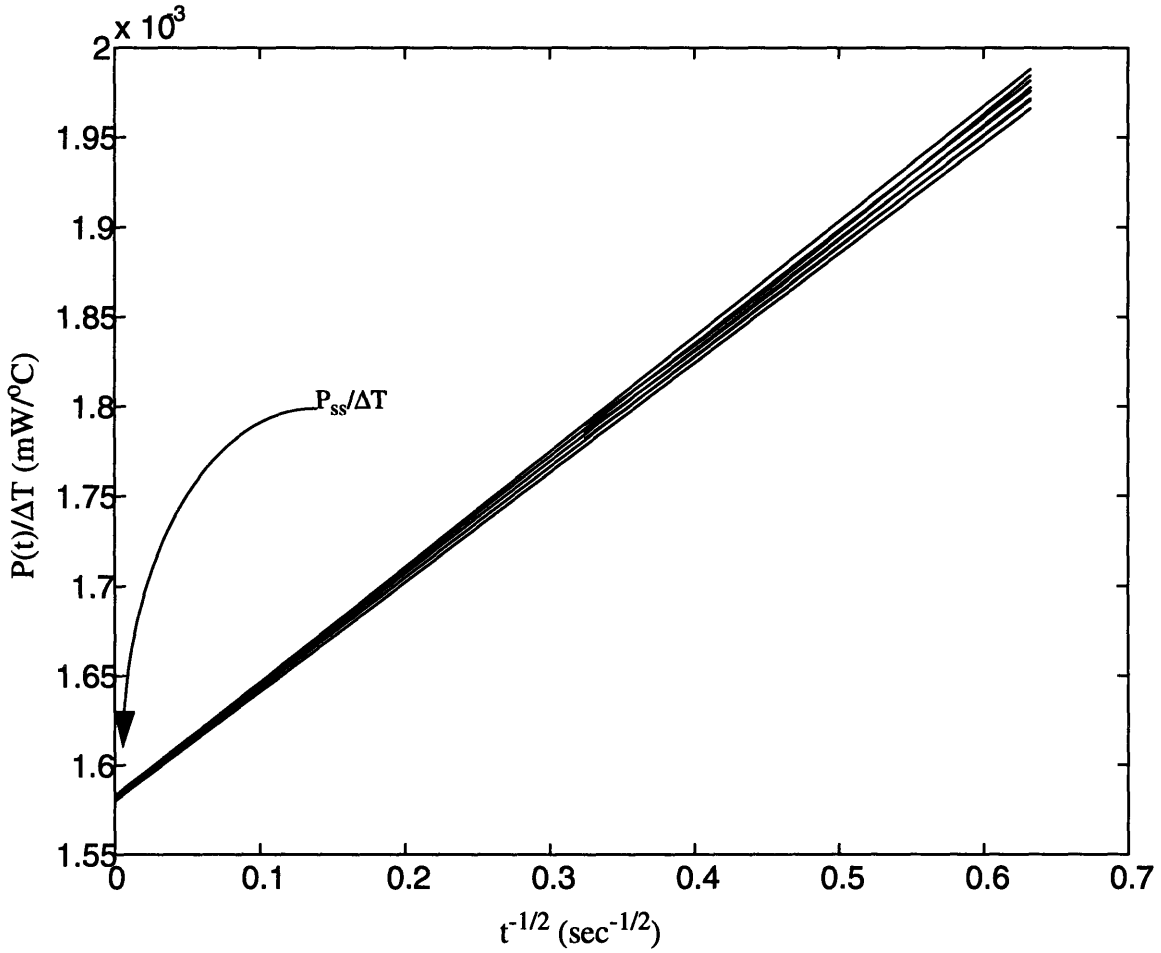

Figure 3.10. The effects of perfusion on the straight line fit to P(t)/ΔT

$P_{ss}/\Delta T$ values for the five curves are all very close to one another, almost on top of each other. This will not be the case if interval five, the 2.5th second to the 39.5th second, of P(t)/ΔT is used for the straight line fit. The $P_{ss}/\Delta T$ values obtained using interval five as the fit interval will show large scatter due to the effects of perfusion corrupting the latter part of the P(t)/ΔT curve.

In order to numerically quantify the effects of perfusion through computer simulation, the same closed form solution of the bioheat equation is implemented and simulated. But rather than have perfusion defined as a constant, perfusion is set to vary with time which is a better approximation to what is really happening. It is assumed to take on

the form of $\omega = 10\sin(2\pi ft + \phi) + 15$. The assumption that perfusion takes on the form of a perfect sinusoid is mostly for simplicity sake and for lack of a better understanding about skin perfusion. The amplitude of the perfusion sinusoid ranges from 5 ml/100gm-min to 25 ml/100gm-min. This is a typical perfusion level range of skin tissue. The phase ϕ is assumed to be a uniform random variable taking on values from 0 to 2π radians. The introduction of a random phase in perfusion accounts for the fact that perfusion is random and that in any particular measurement, it is equally likely to encounter any part of the perfusion sinusoidal wave. The frequency *f* is varied through the gamut of relevant frequencies from 0.01 to 1 Hz. At each frequency setting, 100 simulated thermal conductivity measurements are performed with each taking on a random phase ϕ. For the sake of comparison purposes, the same set of 100 random phase ϕ are used across the board for all the frequency settings. The K_ms from the 100 sets of thermal conductivity measurement data at each frequency is calculated and the percentage errors tabulated. The average K_ms tabulated for each frequency setting are shown on Figure 3.11. The simulated K_m values with perfusion riding on the power response signals seem to oscillate in value from about 3.258 mW/cm-^oC to 3.272 mW/cm-^oC. The true K_m used in the equation for the simulation is 3.2464 mW/cm-^oC. So, for the level of perfusion assumed, it caused roughly 0.4% to 0.8% increase in K_m values. What is even more important is the spread of the simulated K_m values at each frequency setting, which is tabulated and then graphed in Figure 3.12. As shown on the graph, slow perfusion fluctuations of the order of a tenth of a hertz cause the most dramatic effect on the spread of simulated values of K_m. This is intuitively obvious because only 7 seconds worth of $P(t)/\Delta T$ data is used for the straight line fit to extrapolate the value of $P_{ss}/\Delta T$. If the period of the perfusion sinusoid is much larger then 7 seconds, the perfusion sinusoid will appear as some type of dc component riding on top of the $P(t)/\Delta T$ signal causing a straight dc shift in the extrapolated value of $P_{ss}/\Delta T$. If the per-

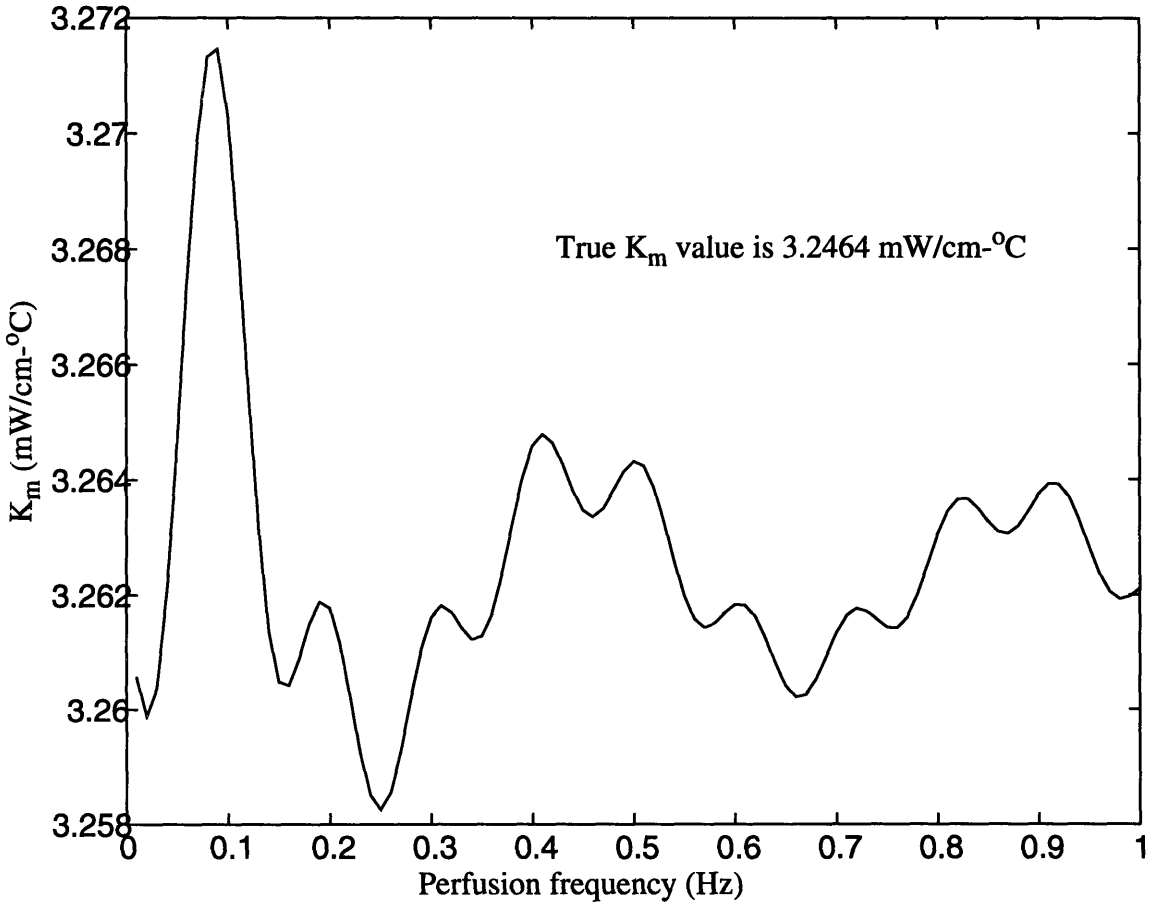

Figure 3.11. The effects of different perfusion frequencies on the value of K_m

fusion sinusoid period is much smaller then 7 seconds, corresponding to frequencies greater than 0.1428 Hz, then the straight line fit will simply average out the fluctuations and diminish the effects of perfusion. In any case, the percent variation due to perfusion is quite substantial. It ranged from a high of nearly 2% to low of 0.2%. Averaged over 0.01 to 1 Hz, perfusion effects cause about 0.6% variability in K_m measurements. Based on this study, conclusion can be drawn that perfusion not only increase the absolute value of measured value of K_m but it also has the potential to introduce large variability in K_m measurements.

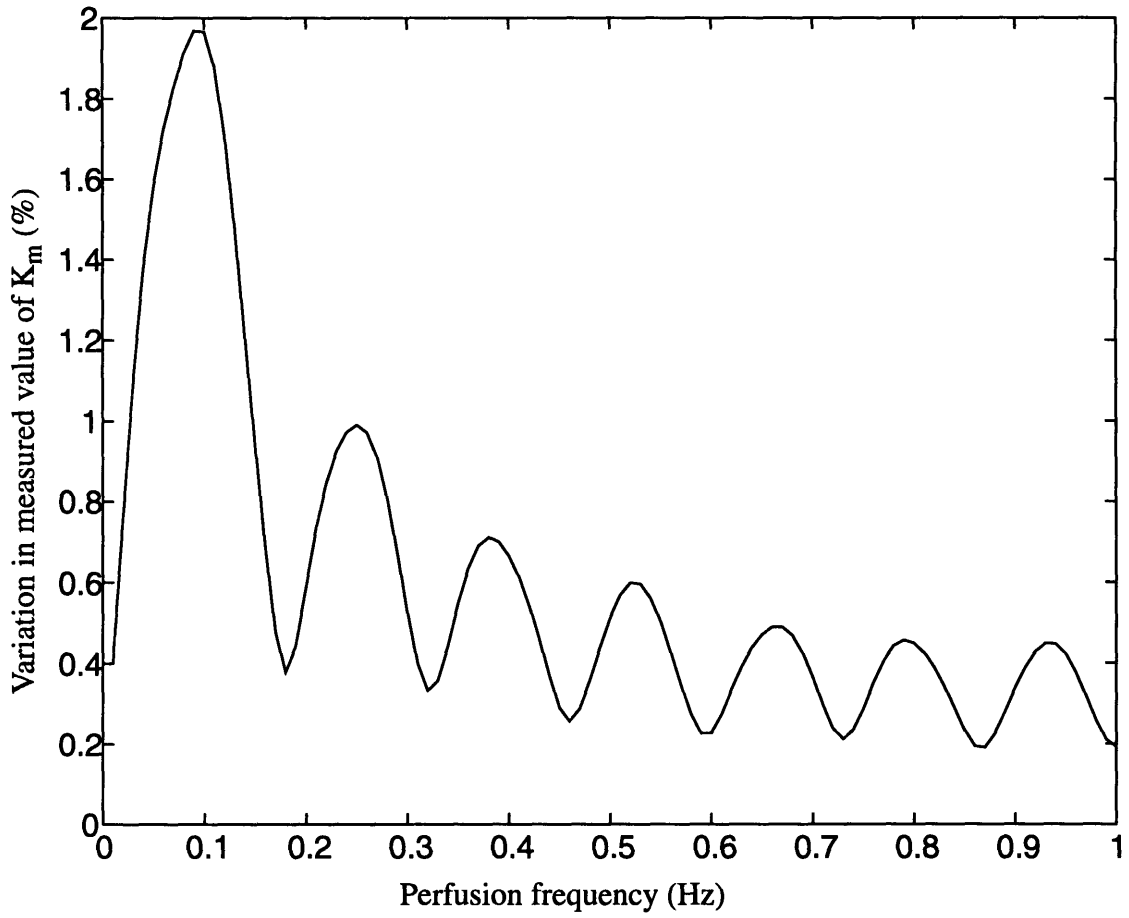

Figure 3.12. The effects of different perfusion frequencies on the variability of K_m

Experimental verification of the effects of perfusion is very difficult due to the difficulty in isolating perfusion effects. Various experiments have been designed and performed in an attempt to quantify the effects. One of the experiments performed involved taking simultaneous skin tissue K_m measurements with a large size thermistor bead and a small size thermistor bead. The large thermistor bead is about 1.2 millimeters in diameter which is 4 times larger then the 0.3 millimeters diameter small thermistor bead. In terms of volume, the large bead is about 64 times larger than the small thermistor bead. The idea behind this experimental approach is that when measurements are performed with a large bead, the tissue volume interrogated by the thermal field is very large in comparison to

that of the smaller bead. Consequently, measurements done with the large size bead should be more prone to perfusion effects and thus have more variability in the data. In contrast, when measurements are performed using a small size thermistor bead, the volume of interrogation is small and hence should be less prone to the effects of perfusion. For the experiment, the two different size beads are placed near one another at about 3 centimeters distance on the skin surface to increase the probability that perfusion variations are approximately the same at each site. If there are inherent intrinsic thermal conductivity changes such as via hydration changes, both beads should be nearly equally effected by it. Figure 3.13 shows the $P(t)/\Delta T$ versus $t^{-1/2}$ curve for skin tissue measure-

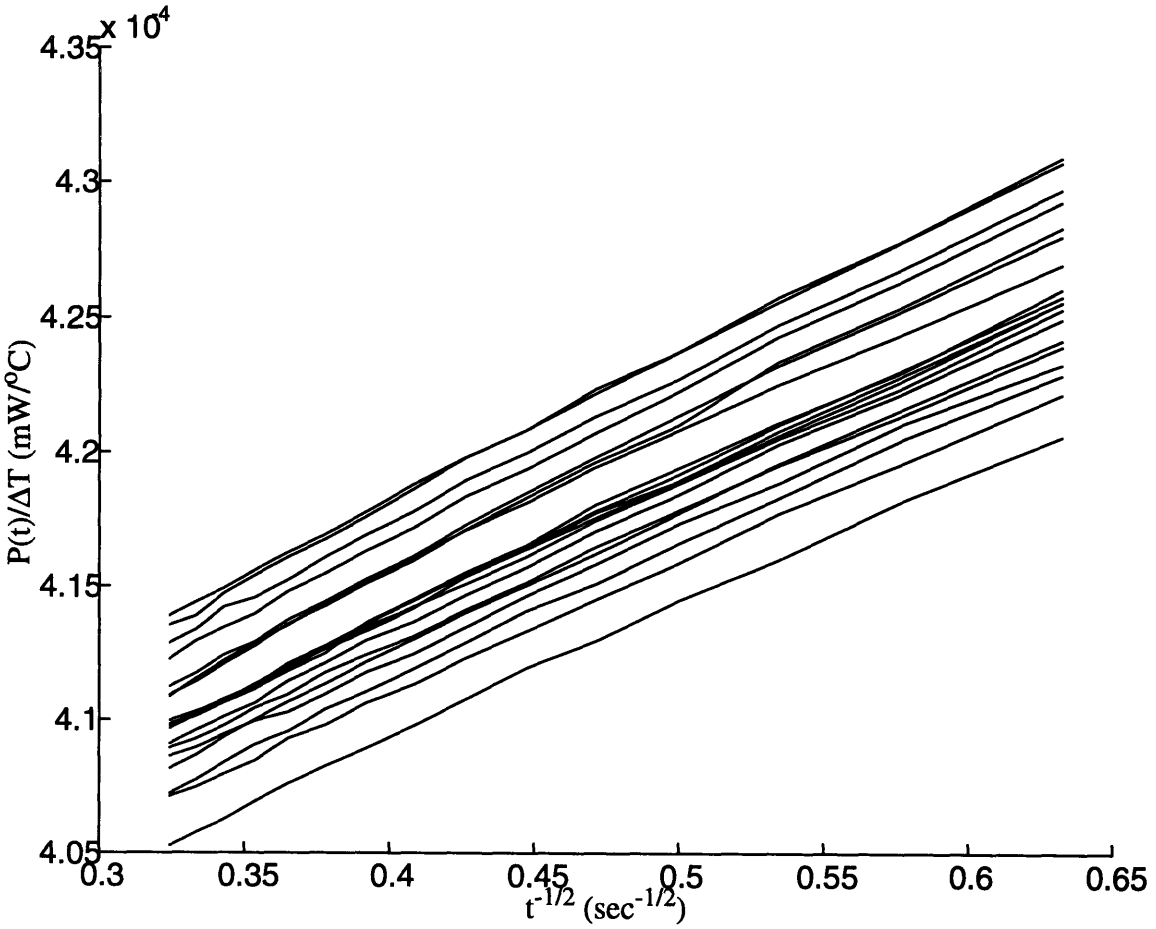

Figure 3.13. Skin tissue K_m measurements using a small size thermistor bead

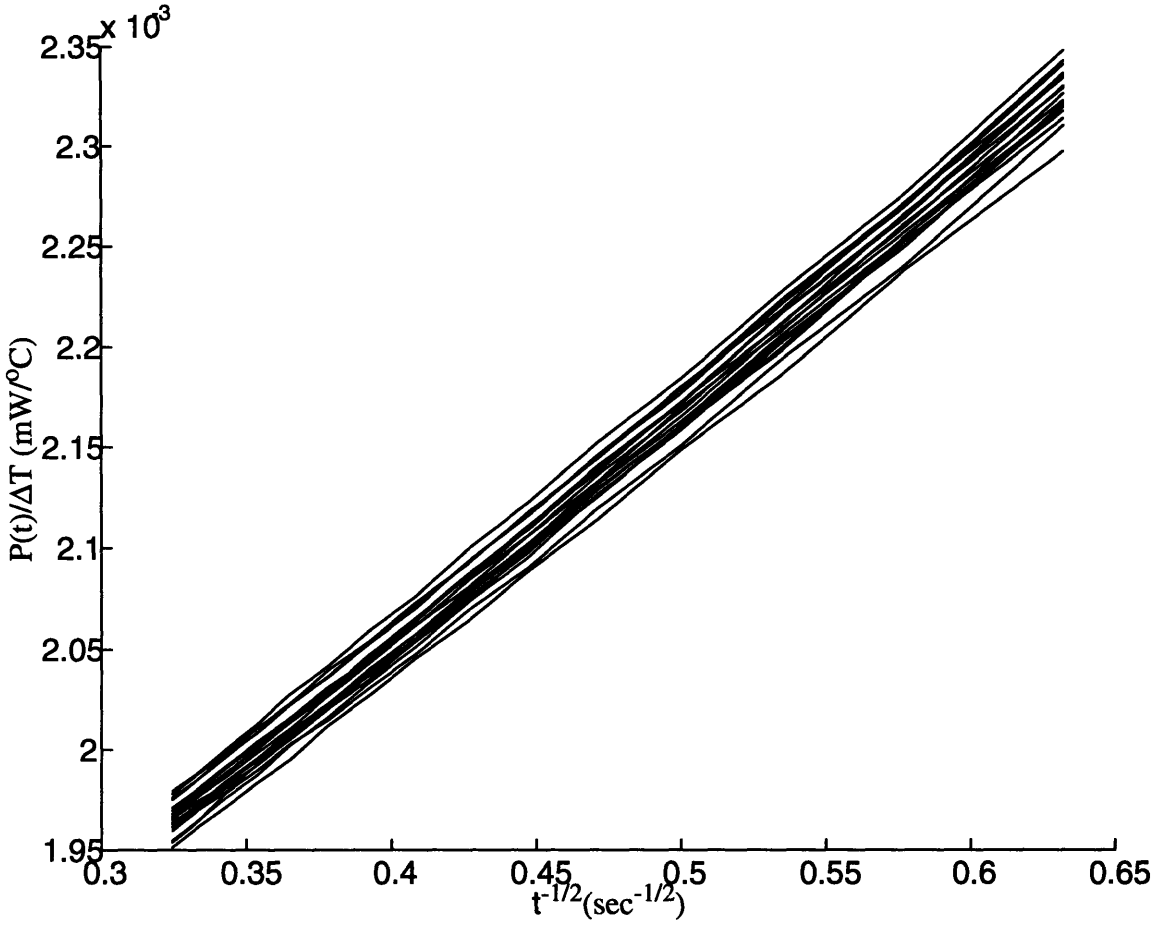

Figure 3.14. Skin tissue K_m measurements using a large size thermistor bead

ments using a small size bead and Figure 3.14 shows the $P(t)/\Delta T$ versus $t^{-1/2}$ curve for skin tissue measurements using a large size bead. The results of this experiment are inconclusive. Even though the simultaneous measurements by the two different size thermistor beads show a smaller spread for the set of measurements done with a smaller size bead, the smaller spread is not statistically significant enough to conclude that the reduction in variability is solely because of the smaller effects of the perfusion.

One of the unexpected problems encountered in this experiment is that the smaller thermistor bead is much more sensitive to temperature variations. Consequently, the baseline temperature as sensed by the smaller bead have a larger variation. This leads

to larger errors. So, by using a smaller thermistor bead, the effects of perfusion might be reduced leading to lower variability. But on the other hand, the smaller thermistor bead maybe more sensitive to baseline temperature fluctuations leading to higher variability in K_m measurements. It is because of this inability to isolate perfusion effects and other sources of variability that has made experimental confirmation of perfusion effects difficult.

3.5 Probe-Tissue Contact

The thermal technique utilized by the TDP200 for thermal conductivity measurements relies on the idea of known heat generation in a calibrated probe, transfer of said heat to a medium, and dissipation of that heat within the medium. Heat transfer from the probe depends heavily on the quality of the contact between the thermistor probe and the medium being measured. The TDP200 assumes that this thermal contact is perfect. Perfect in the sense that under the same conditions, the measurements would be identical, that there are no air bubbles or air films formed between the probe and the medium to impede the transfer of the heat between the thermistor bead and the skin. Microscopic air bubbles/air films serve as insulators and dampen the effectiveness of the heat transfer. Indeed the heat transfer coefficient is both degraded and variable. A perfect contact criterion would require the entire measuring surface of the thermistor bead to be in intimate thermal contact with the medium. This usually would require a wetted surface. However, non-wetted probe/tissue interface of constant contact pressure would also give consistent results.

Thermal conductivity measurements performed in agar gels or glycerol mixture gels do not suffer from probe contact problems. This is because prior to performing K_m measurements, the surface mount thermistor probe is situated in either liquid agar or liquid glycerol mixture before they are solidified. As a free flowing liquid, these media

flows around and makes good thermal contact between the probe and media. Once the liquid gel solidifies, the contact between the thermistor probe and the gel is near perfect and contact problems are effectively eliminated. The thermal field generated by the bead is quite symmetrical when dealing with homogeneous media. The symmetric distribution of the thermal field is in accordance with the assumption made when solving for the solution to the bioheat equation.

Various factors prevent perfect surface contact to exist between the measuring thermistor probe and skin tissue. The skin tissue surface is microscopically very uneven permitting pockets of air to exist at the interface. To quantify the impact of this non-ideal contact between the thermistor bead and the skin surface, a controlled experiment was performed on a piece of beef. The piece of beef was used to simulate the geometric surface conditions of skin tissue without the problems associated with surface skin tissue measurements such as baseline temperature fluctuations, perfusion effects, and inherent hydration induced K_m changes. Invasive K_m measurements are performed to serve as a control. The invasive probe is introduced into the beef specimen by way of an angiocath. Surface K_m measurements served as the variable part of the experiment. The surface probe is placed on top of the beef near the location of the invasive probe. This experimental setup is shown in Figure 3.15. The tissue paper underneath the beef is used to absorb water leaking from the beef tissue as it is heated to 37.3°C. Once the temperature of the beef stabilizes to 37.3°C, twenty K_m measurements are made simultaneously by both the invasive and surface probes. The results show that the percent variability in the invasive measurements is 0.15%. Typical invasive measurements performed on agar and glycerol mixture gels usually show percent variability of around 0.2% in K_m. This is about the TDP200's precision limit. Since the percent variations obtained while making K_m measurements invasively in beef tissue is consistent with expectations, it can be inferred that the experi-

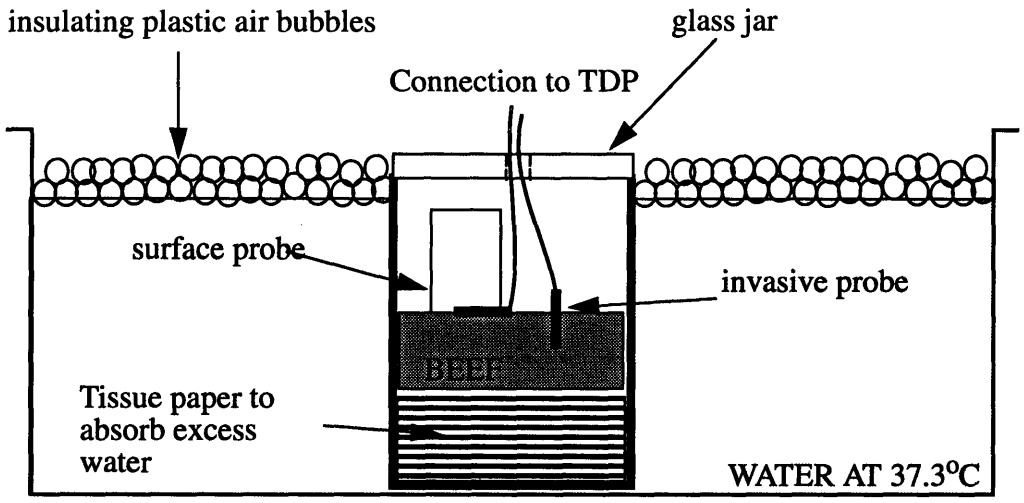

Figure 3.15. Experimental setup for investigating probe-tissue contact problems

mental setup is not subject to outside sources of errors. The results of K_m measurements performed on the surface of the beef tissue show a percent variability of 0.81%. This is a 0.66% increase as a result of changing the contact configuration of the K_m measurements from invasive to non-invasive surface contact. By making the reasonable assumption that the 0.15% variability of invasive K_m measurement is the precision limit of the TDP200 and that the probe contact error is independent of the precision limit error, it can be back calculated that probe contact problem gives rise to 0.8% variability in surface K_m measurements. Based on this beef tissue data, it can be concluded that surface contact between the thermistor probe and the skin tissue is a large source of variability in K_m measurements. Various attempts have been made to minimize the contact problem. For instance, thermally conductive gels composed of water and glycerol have been applied between the surface probe and the skin tissue to stop the formation of air bubbles and air films, and hence improve contact. The use of contact gels show promise but does not fully solve the contact problem particularly for irregular surface geometry during measurements.

There is another potential source of error associated with surface probes. When the probe is placed on the skin surface, it is not very securely fastened to the surface, and is very sensitive to random relative movements at the skin/probe interface. These movement errors are generally discernible as motion artifact.

3.6 Dependence of K_m on ΔT

The derived value of $P_{ss}/\Delta T$, based on the TDP200 measured data, directly determines the value of the skin tissue intrinsic thermal conductivity K_m. Ideally for a given K_m, this extrapolated value is independent of the applied temperature step. If the temperature step is increased or decreased, the value of P_{ss} changes to offset the effect of the changing ΔT. The ratio of $P_{ss}/\Delta T$ should be maintained constant independent of ΔT. However, that is not found to be the case. The ratio of $P_{ss}/\Delta T$ varies as a function of ΔT and this causes some difficulty in establishing the true value of the skin tissue K_m. On repetitive runs of skin tissue measurements, the values of ΔT vary quite a bit because of the finite steps of available ladder resistance. This variability of ΔT translates to variability in $P_{ss}/\Delta T$, which means variability in skin tissue K_m. Repetitive K_m measurements show variability in ΔT because the baseline temperature T_o used for each of the repetitive runs varies with time. For each different value of T_o in the set of repetitive runs, the TDP200 tries to set T_{heat} to achieve the same ΔT for all the repetitive runs. However, as mentioned, the resistor ladder that determines T_{heat} is only of finite precision. It can only take on certain predetermined values. So when ΔT is the difference between T_{heat} and T_o, and T_{heat} can only have a finite number of values while T_o can vary continuously, the end result is variations in ΔT. In a typical set of runs, the percent variability of ΔT maybe 2%. The question is how much percent variability in K_m results for every percent variability in ΔT.

To answer this question, the exact dependence of $P_{ss}/\Delta T$ on ΔT must first be found. Two static media are used to carry out this investigation - agar gel with 100% agar

having K_m of 6.23 mW/cm-°C, and glycerol mixture gel with 80% glycerol and 20% agar having K_m of 3.35 mW/cm-°C. The same surface thermistor probes are placed on the two gels and K_m measurements are performed using varying size ΔT from 1 °C to 10 °C. 190 K_m measurements are performed on each static medium with each repetitive run done 6 minutes apart to allow for thermistor probe cooling. The baseline temperature T_o and T_{heat} temperature profiles for the 190 measurements in agar gel are shown in Figure 3.16. Like-

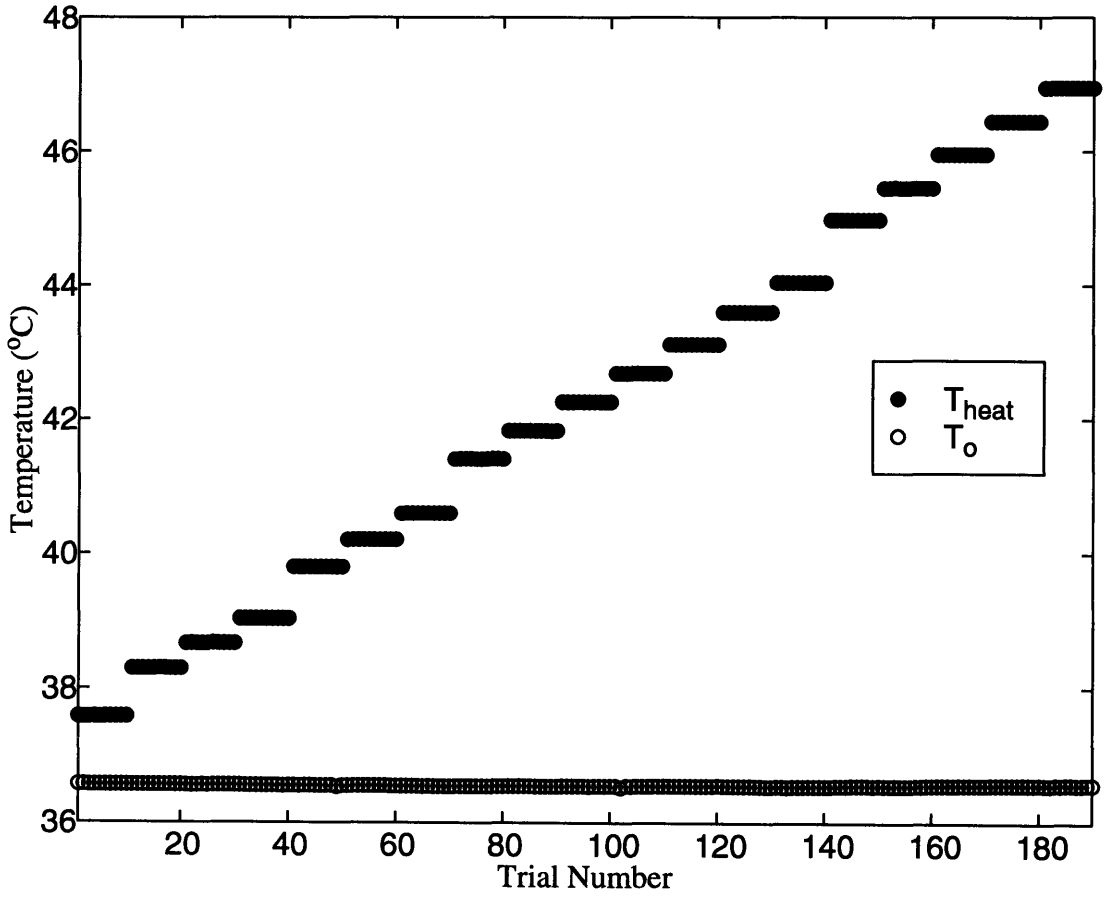

Figure 3.16. T_o & T_{heat} temperature profiles of 190 agar variable ΔT experiments

wise, Figure 3.17 shows the T_o and T_{heat} temperature profiles for the 190 measurements done in the agar-glycerol mixture gel. The ΔT profiles of the experiments are simply the difference between the heat temperature T_{heat} and the baseline temperature T_o of the bead.

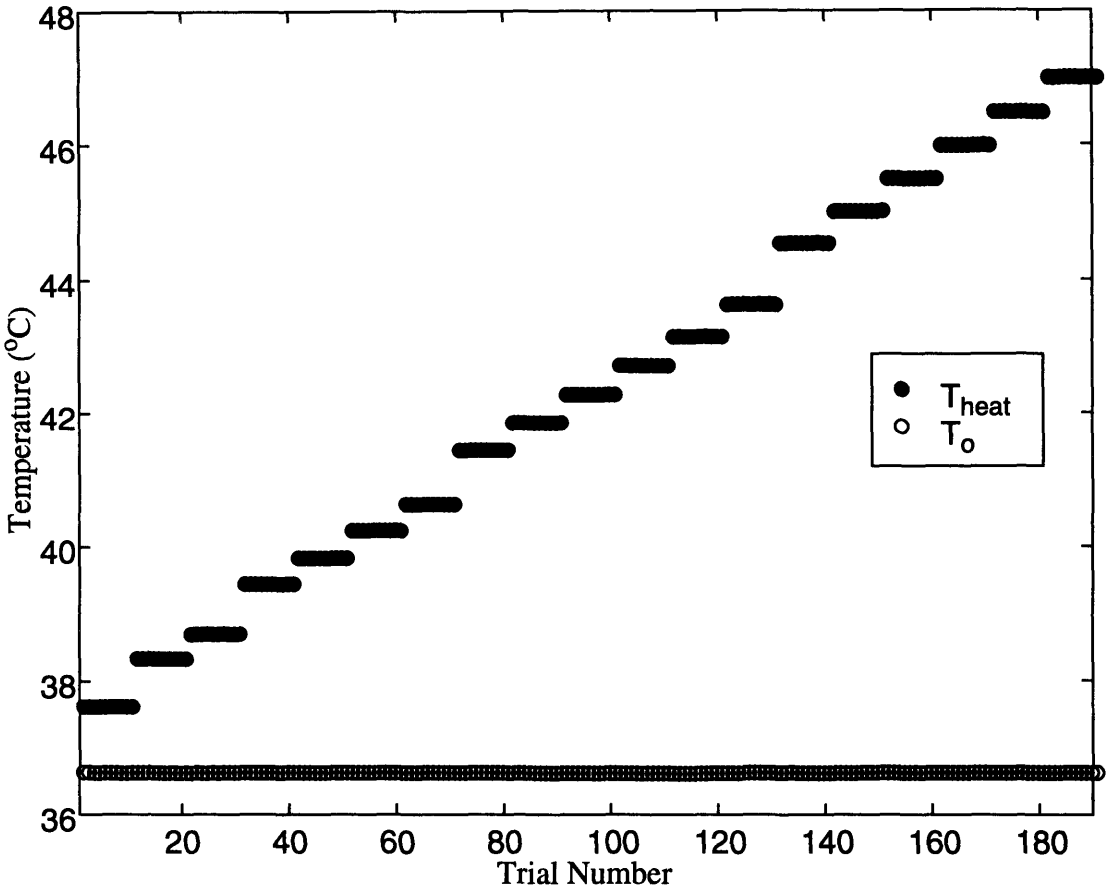

Figure 3.17. T_o & T_{heat} temperature profiles of 190 glycerol mix variable ΔT experiments

It is well known that the thermal conductivity K_m of the two gels have a positive temperature coefficient and therfore rise with baseline temperature, so to keep the baseline T_o constant throughout the experiments, the two static gels are placed in a water bath to ensure constant T_o. In the experiment, ΔT is increased at a step size of roughly 0.5°C starting at around ΔT = 1 °C. At each ΔT setting, ten K_m measurements are performed. Figures 3.18 and 3.19 show the 190 derived values of $P_{ss}/\Delta T$ from the K_m measurements done in agar and glycerol mixture gels respectively. It is important to note from the figures that regardless of what the testing medium is, the derived values of $P_{ss}/\Delta T$ are increasing meaning

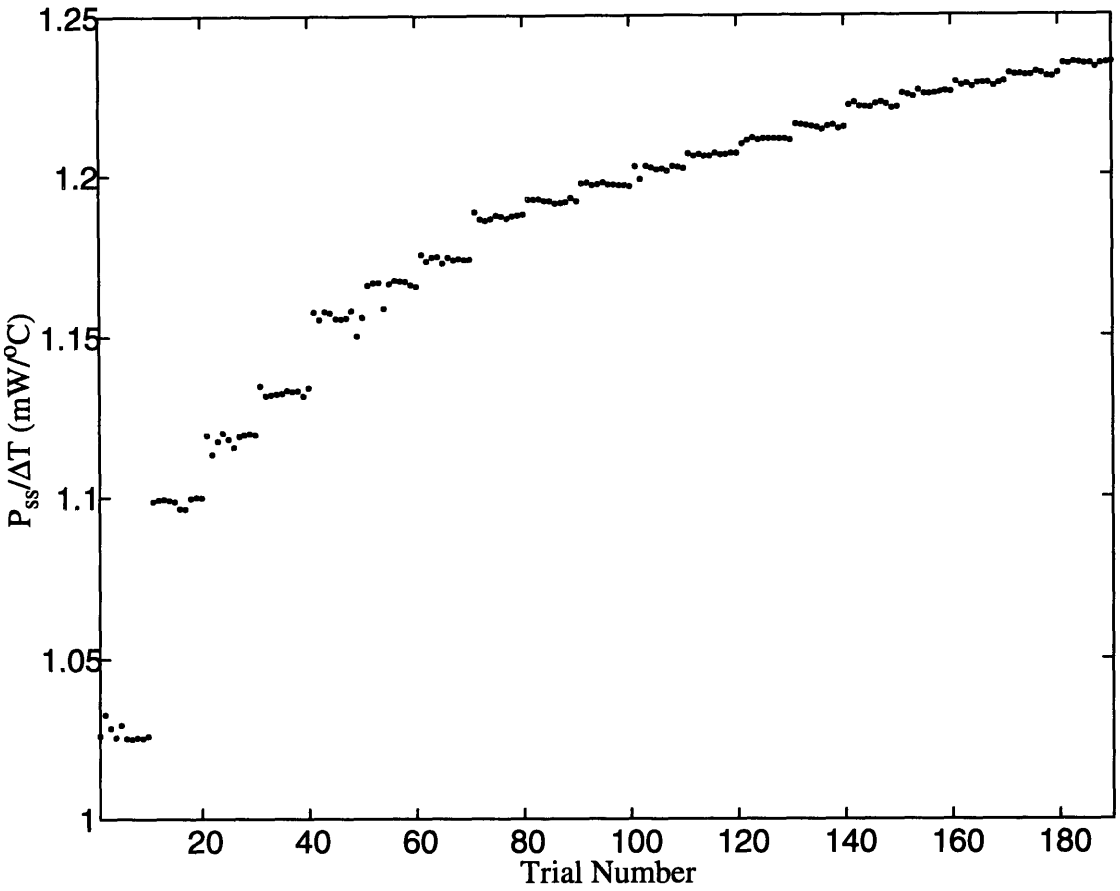

Figure 3.18. $P_{ss}/\Delta T$ values of 190 variable ΔT experiments in agar gel

that the experimental values of K_m are increasing. This contradicts the 1st order assumption that K_m values for the gels are constant. The derived values of $P_{ss}/\Delta T$ are plotted against the applied temperature step ΔT in Figure 20. The plot shows that the derived values of $P_{ss}/\Delta T$ increase logarithmically with increasing ΔT. Ideally, this plot should show two horizontal lines intersecting the $P_{ss}/\Delta T$ axis at two different values with each value representing the correct K_m value of the gel. To realize just how values of $P_{ss}/\Delta T$ varies with ΔT for each of the two testing media, a two exponential curve is fitted to the plot of $P_{ss}/\Delta T$ versus ΔT for each testing medium. The two exponential curve fits are done by

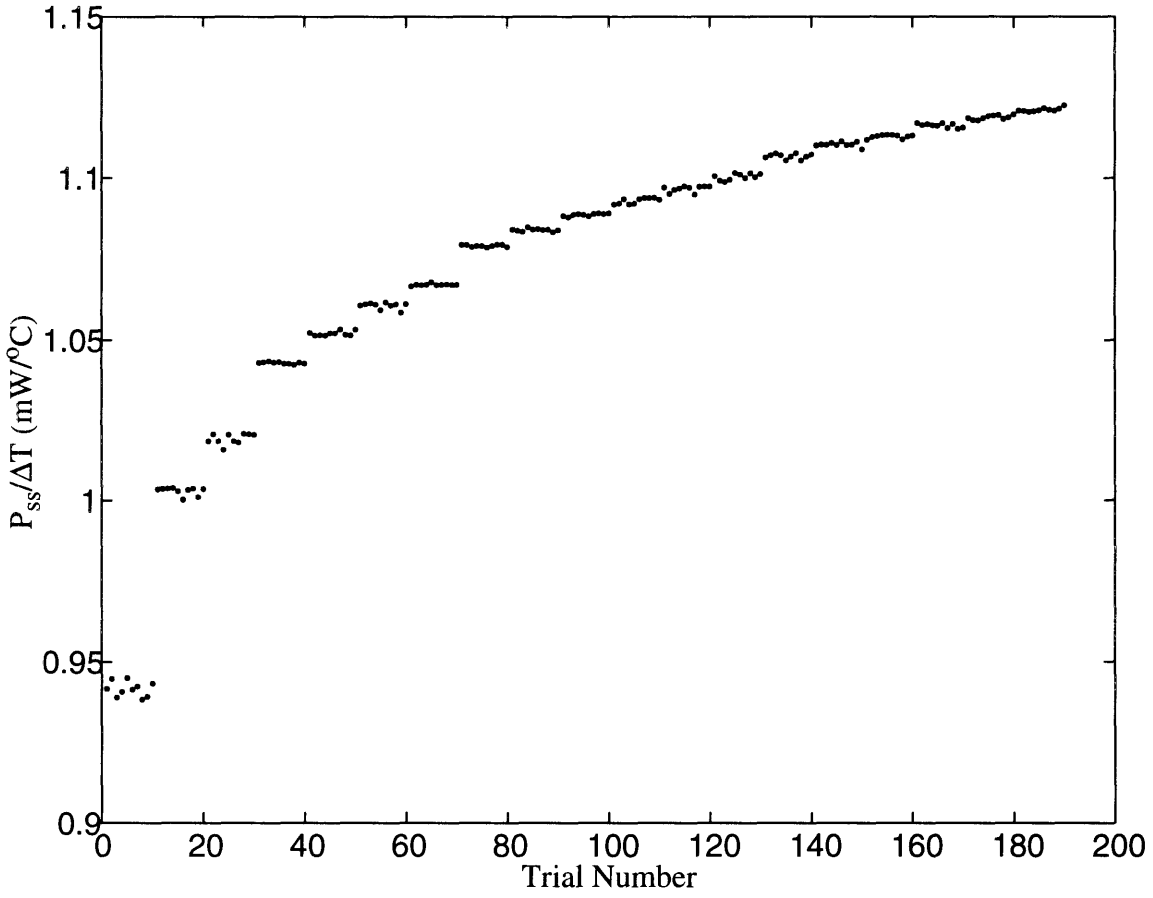

Figure 3.19. $P_{ss}/\Delta T$ values of 190 variable ΔT experiments in glycerol mixture gel

using Gauss-Newton's least squares method with cubic interpolation. The results of the curve fitting show that in agar, the relationship between $P_{ss}/\Delta T$ and ΔT is

$$\frac{P_{ss}}{\Delta T} = -0.3115e^{-0.823\Delta T} + 1.155e^{0.006557\Delta T} \quad . \tag{3.7}$$

In glycerol mixture, the relationship between $P_{ss}/\Delta T$ and ΔT is

$$\frac{P_{ss}}{\Delta T} = -0.2563e^{-0.8011\Delta T} + 1.053e^{0.00628\Delta T} \quad . \tag{3.8}$$

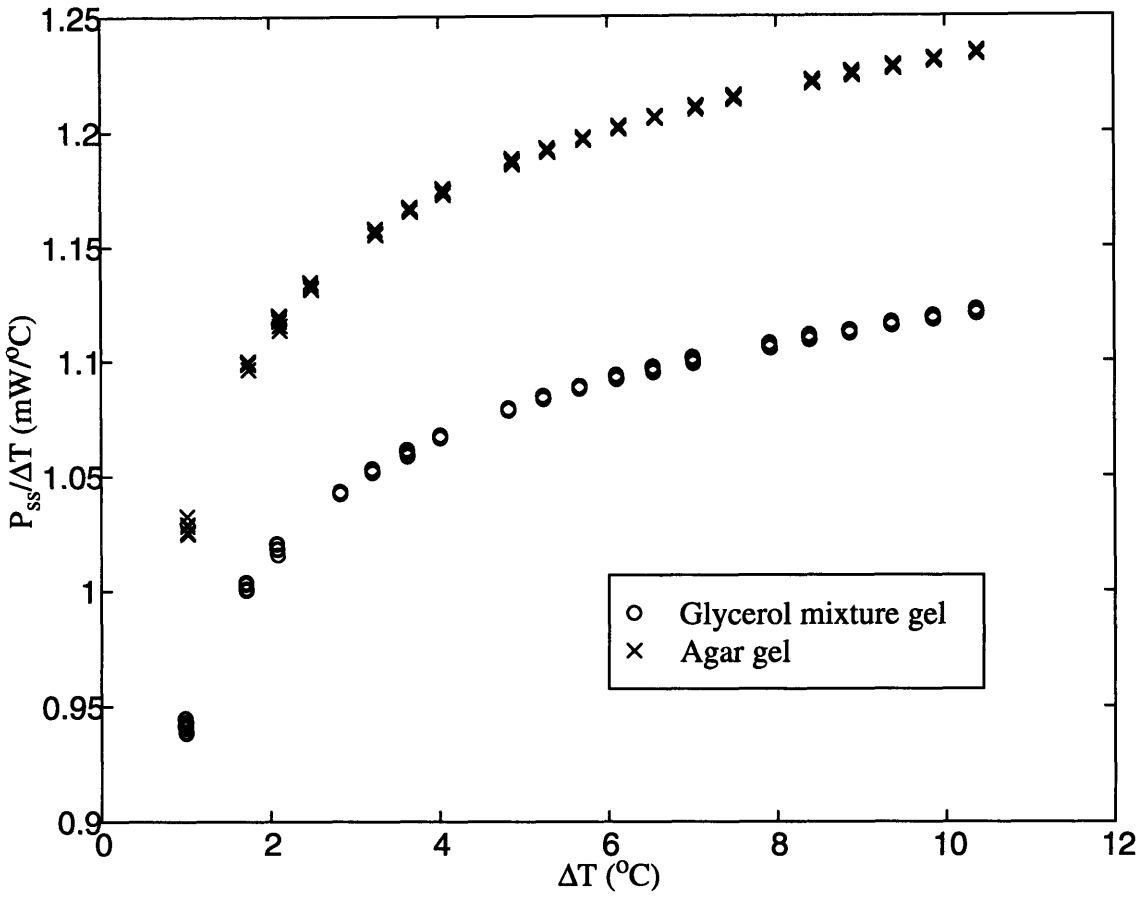

Figure 3.20. Demonstration of $P_{ss}/\Delta T$ dependence on ΔT in the variable ΔT experiments

Since the skin tissue intrinsic thermal conductivity is closer in value to the K_m value of the glycerol mixture, equation 3.8 is used to estimate the percent variation of $P_{ss}/\Delta T$ due to variations in ΔT of skin tissue. By taking the partial derivative of equation 3.8 with respect to ΔT and dividing the result by $P_{ss}/\Delta T^2$, the following relationship is obtained:

$$\frac{\frac{\partial\left(P_{ss}/\Delta T\right)}{P_{ss}/\Delta T}}{\frac{\partial \Delta T}{\Delta T}} = \frac{\%\text{var}\, P_{ss}/\Delta T}{\%\text{var}\, \Delta T} = \frac{\left(0.2053e^{-0.8011\Delta T} + 0.0066128e^{0.00628\Delta T}\right)\Delta T}{-0.2563e^{-0.8011\Delta T} + 1.053e^{0.00628\Delta T}}. \quad (3.9)$$

Using equation 3.9 and values consistent with skin tissue measurements, $\Delta T = 6$ °C, it is found that every percent variability in ΔT gives rise to 0.047% variability in $P_{ss}/\Delta T$. A

relationship must be obtained in order to translate from percent variability in $P_{ss}/\Delta T$ to percent variability in K_m. The relationship can be obtained by taking the partial derivative of equation 3.1 with respect to $P_{ss}/\Delta T$ and dividing the result by $\frac{P_{ss}/\Delta T}{K_m}$.

$$\frac{\frac{\partial K_m}{K_m}}{\frac{\partial P_{ss}/\Delta T}{P_{ss}/\Delta T}} = \frac{\%\text{var } K_m}{\%\text{var } P_{ss}/\Delta T} = 1 + \frac{K_m}{5K_b} \tag{3.10}$$

Again, using values consistent with skin tissue measurements, $K_m = 3.35$ mW/cm-^oC, and $K_b = 0.1617$ mW/cm-^oC, gives 4.55% variability in K_m for every percent variability in $P_{ss}/\Delta T$. To relate percent variability in ΔT to percent variability in K_m, equations 3.9 and 3.10 are combined to obtained the following relationship.

$$\frac{\%\text{var } K_m}{\%\text{var } \Delta T} = \left(1 + \frac{K_m}{5K_b}\right) \cdot \left(\frac{\left(0.2053e^{-0.8011\Delta T} + 0.0066128e^{0.00628\Delta T}\right)\Delta T}{-0.2563e^{-0.8011\Delta T} + 1.053e^{0.00628\Delta T}} \right) \tag{3.11}$$

So, for example, if a typical 2% variation in the ΔT occurs in a set of repetitive skin tissue measurements where $K_m = 3.35$ mW/cm-^oC and $K_b = 0.1617$ mW/cm-^oC, approximately 0.4% variability in the measured values of K_m results.

A possible explanation for why $P_{ss}/\Delta T$ is a function of ΔT lies in the resistance of the heat thermistor bead. As the ΔT applied to the thermistor bead increases, the increase in heat in the bead causes the thermistor resistance to decrease. This effect is observed in all types of resistors. As the thermistor resistance decreases and the voltage applied across it is maintained the same, the power given to the thermistor bead is going to increase. The increase in power causes further heating of the thermistor bead causing the thermistor resistance to again decrease in value. This positive feedback cycle continues and is not taken into account by the TDP200. As a result, with increasing temperature

step, the P_{ss} is going to increase more then proportionally leading to an increase in the ratio $P_{ss}/\Delta T$. The logarithmic behavior of $P_{ss}/\Delta T$ versus ΔT is expected. The resistance versus heating of a typical resistor looks very much like a decaying exponential. At low heating, corresponding to small ΔT, thermistor resistance decrease substantially forcing substantial increase in P_{ss}. As the heating becomes more intensive, corresponding to larger ΔT, the thermistor resistance decreases but at a slower rate forcing smaller increases in P_{ss}. Based on this discussion, $P_{ss}/\Delta T$ is going to increase substantially at low ΔT and the rate of increase is going to decreases as ΔT increases. In other words, $P_{ss}/\Delta T$ is going to increase logarithmically with ΔT.

A way of correcting for the $P_{ss}/\Delta T$'s dependence on ΔT is to make the calibration constants K_b and a functions of ΔT hence they can be used to offset ΔT effects. Essentially, the role of $K_b(\Delta T)$ and $a(\Delta T)$ is to warp the two logarithmic curves shown in Figure 3.20 into two horizontal line thus making K_m independent of ΔT. At each of the different settings of ΔT, different sets of $K_b(\Delta T)$ and $a(\Delta T)$ are found to ensure that each of the different $P_{ss}/\Delta T$ values found in the two media maps to the correct K_m values. For instance at $\Delta T = 5\ ^oC$, $K_b(5)$ and $a(5)$ are found with the aid of equation 3.1 so that the $P_{ss}/\Delta T$ values obtained from agar gel and glycerol mixture gel can be correctly translated to K_m values of 6.23 mW/cm-^{o}C and 3.35 mW/cm-^{o}C respectively. It is important to note that two different static media are required for finding the two calibration constants. 190 experimental sets of $K_b(\Delta T)$ and $a(\Delta T)$ are found using the above method. A two exponential curve is fitted to these data sets of $K_b(\Delta T)$ and $a(\Delta T)$ using Gauss-Newton's least squares method with cubic interpolation. Only a two exponential curve is generated for the fit therefore, the result of the curve fit may not be entirely correct. More exponential terms may be added in for the fit to increase the accuracy. The resulting two exponential $K_b(\Delta T)$ and $a(\Delta T)$ found are shown in equations 3.12 and 3.13.

$$K_b(\Delta T) = -0.07885e^{-1.163\Delta T} + 0.1852e^{0.003203\Delta T} \tag{3.12}$$

$$a(\Delta T) = 0.2552e^{-2.717\Delta T} + 1.122e^{0.005836\Delta T} \tag{3.13}$$

Presently, the TDP200 uses one set of fixed K_b and a constants that are obtained with $\Delta T = 6\ ^{o}C$. With this method, the values of $P_{ss}/\Delta T$ obtained in the variable ΔT experiment are translated to K_m values via equation 3.2. These K_m values are plotted against ΔT as shown in Figure 3.21. Notice that the K_m values of both agar gel and glyc-

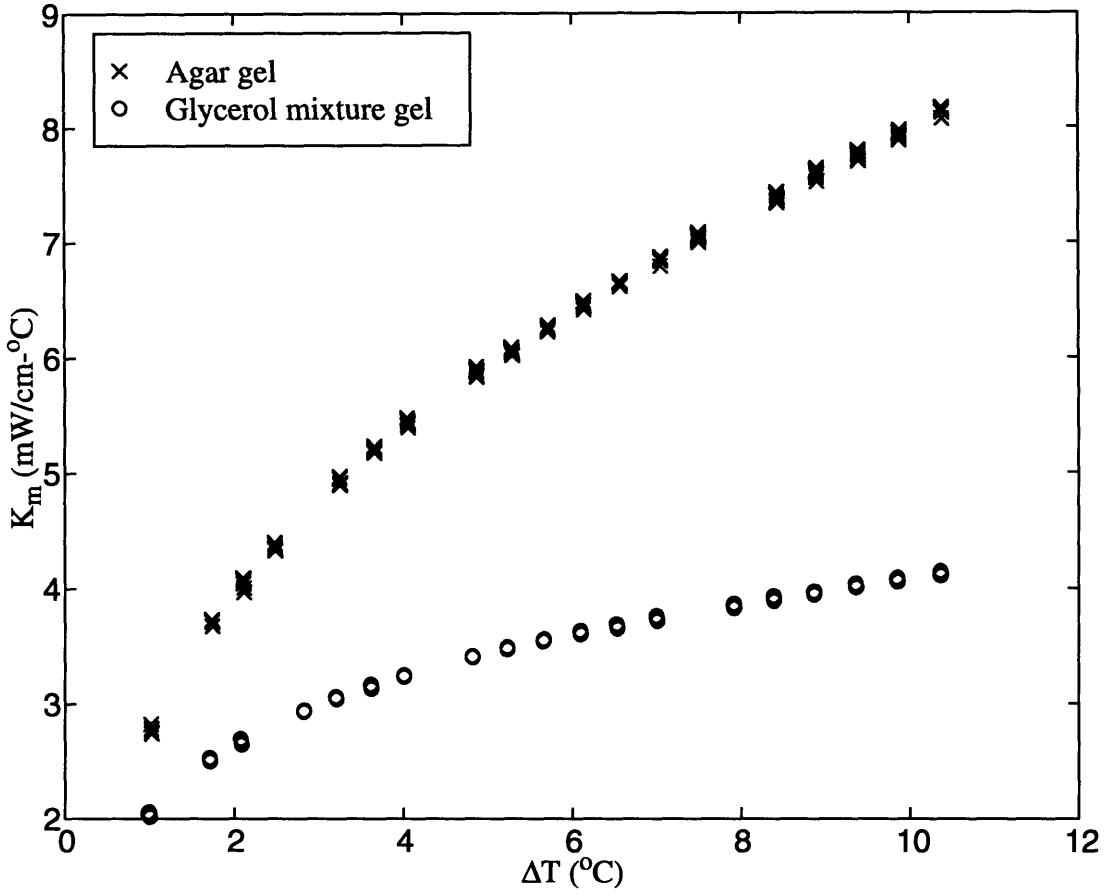

Figure 3.21. Illustration of the functional dependence of K_m on ΔT

erol mixture gel vary substantially. The agar gel's K_m values change from about 3 mW/

cm-^{o}C to over 8 mW/cm-^{o}C. Similarly, the glycerol mixture gel's K_m values increase from 2 mW/cm-^{o}C to over 4 mW/cm-^{o}C. In contrast, when ΔT dependent $K_b(\Delta T)$ and $a(\Delta T)$ calibration constants are used to translate from $P_{ss}/\Delta T$ to K_m via equation 3.1, the K_m values of the gels are much more constant. This is shown in Figure 3.22.

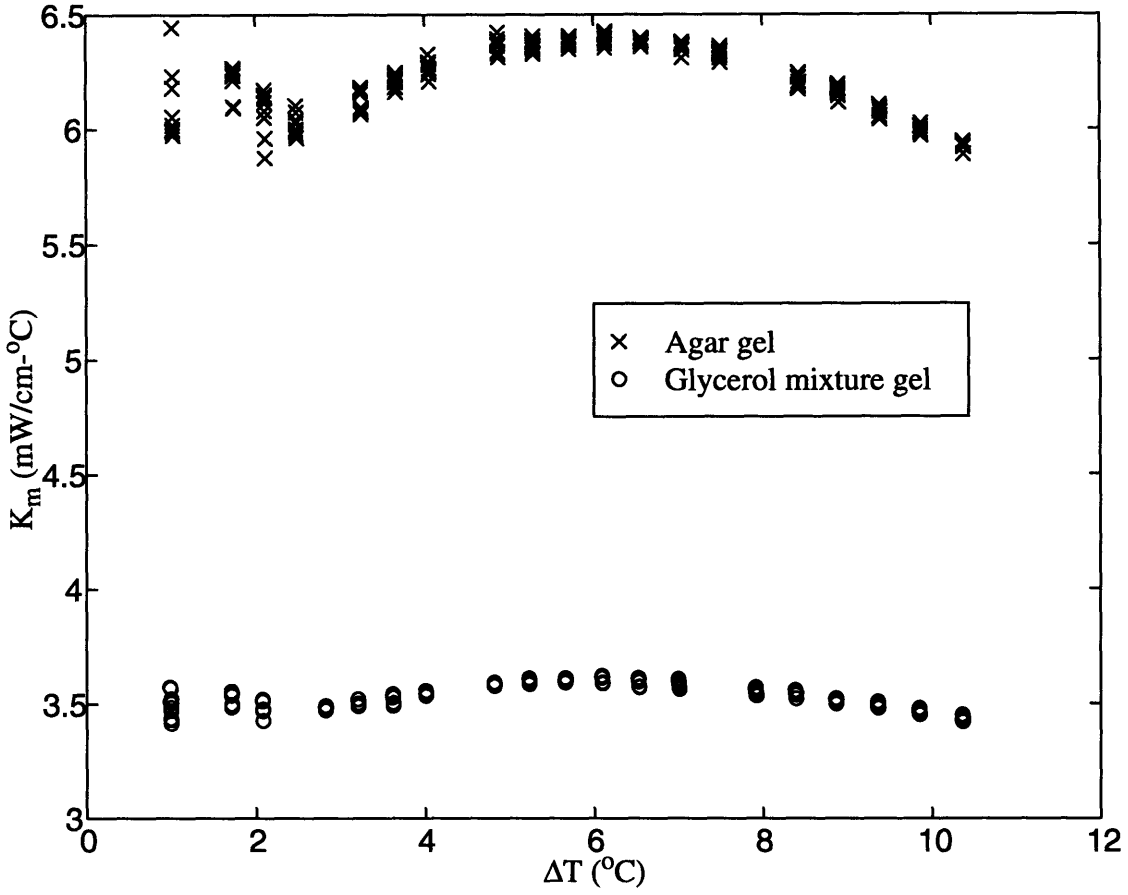

Figure 3.22. Result of using $K_b(\Delta T)$ and $a(\Delta T)$ to correct for K_m dependence on ΔT

On a particular set of skin tissue K_m measurement data with ΔT variability of 2%, the new algorithm of using $K_b(\Delta T)$ and $a(\Delta T)$ show a 0.3% improvement in K_m variability over the old algorithm of using constant K_b and a. With a 2% variability in ΔT, equation 3.12 predicts a 0.4% variability in K_m. The new algorithm is unable to entirely correct for this 0.4% variability in K_m as a result of ΔT variations. This is because the

dependence of $P_{ss}/\Delta T$ on ΔT is roughly estimated by a two exponential curve. In addition, the $K_b(\Delta T)$ and $a(\Delta T)$ that are part of the solution are also roughly estimated by a two exponential curve. The real underlying dependence of $P_{ss}/\Delta T$, $K_b(\Delta T)$ and $a(\Delta T)$ on ΔT are unknown. It is due to this rough estimate that the new algorithm is unable to adjust and totally correct for all the variability in K_m due to variations in ΔT. The imperfect estimate of $P_{ss}/\Delta T$, $K_b(\Delta T)$, and $a(\Delta T)$ can be further observed in Figure 3.22. Notice that even though the K_m values found for all ΔT with the new algorithm are much more in line with what was expected as compared to ones obtained with the old algorithm shown on Figure 3.21, the K_m values are still by no means entirely constant. As shown in Figure 3.22, the K_m values for both agar gel and glycerol mixture gel waver in value. This again is due to the rough estimate of the dependence of $P_{ss}/\Delta T$ on ΔT and also on the rough assessment of $K_b(\Delta T)$ and $a(\Delta T)$. If there is a way of gaining insight to know the exact dependence of $P_{ss}/\Delta T$ on ΔT and a way of perfectly evaluating $K_b(\Delta T)$ and $a(\Delta T)$, then Figure 3.22 will show flat horizontal lines demonstrating constant K_ms for both agar gel and glycerol mixture gel for all ΔT used. In this case, the new algorithm can be used to entirely correct for the variation in K_m due to variations in ΔT.

3.7 Hydration Induced K_m Variations

One argument for observing variability in skin tissue intrinsic thermal conductivity is that the observed variations may actually be inherent changes in the thermal conductivity of skin tissue. Inevitably, through the course of time, the skin tissue thermal conductivity of human beings is going change. The reason for this natural change may be due to shifts in the composition of skin tissue. Skin tissue is composed of approximately 64.68% water, 0.68% ash, 13% crude fat, and 22.19% crude protein. Water is a major constituent of skin tissue and at the same time, has a high thermal conductivity value of 6.23 mW/cm-^{o}C. Ash, crude fat, and crude protein all have low thermal conductivity values

and all play a small part in the make up of skin tissue. As a result, water plays a dominant role in determining the thermal conductive nature of skin tissue. Skin tissue water content change as a result of osmotic pressure caused by blood perfusion. For instance, high levels of perfusion in the blood vessels of skin tissue force higher amount of fluid to enter the adjacent skin tissue leading to higher water content. Skin tissue with higher water content leads to higher intrinsic thermal conductivity. And since perfusion phenomenon is quite random in nature, this causes the water level of the skin tissue to shift randomly as well, meaning that intrinsic thermal conductivity fluctuates randomly too.

Time will elapse over a set of skin tissue intrinsic thermal conductivity measurements. Typically in a set of twenty measurements, it takes roughly 2 hours to collect. In this 2 hour time frame, it is more than likely that perfusion levels are going to change and affect the water content of the skin tissue leading to changes in the skin tissue K_m. Due to the inability to predict the perfusion level of skin tissue and the lack of knowledge on the relationship between perfusion and water content changes in skin tissue, it is difficult to get a handle on just how much skin tissue thermal conductivity can change over time. A better understanding of the fundamentals of this problem can lead to formulation of hypotheses with well thought out experiments to quantify this change. But before that can be accomplished, this question remains unanswered.

Chapter 4

Conclusions

The intent of this thesis is to provide an explanation and possible solutions for why the Thermal Diffusion Probe 200 is able to measure the K_m of phantoms with less then 0.2% accuracy while not achieving this same level of reproducibility on skin tissue K_m measurements. Several possible major sources of variability are identified as part of the investigation - low sampling rate, skin tissue baseline fluctuations, random perfusion effects, probe-tissue thermal contact problems, dependence of $P_{ss}/\Delta T$ on ΔT, and inherent hydration induced changes in skin tissue intrinsic thermal conductivity. Each source of variability is closely examined to quantify its effects. The precision limit of the TDP200 is established by taking measurements on phantom materials where the K_m is precisely known and is constant for the duration of the measurement. The low sampling rate of the TDP200 is first speculated to be a major source of variability. The 2 Hz sampling frequency is thought to be adequate in representing possible high frequency components of the $P(t)/\Delta T$ curve. However, after increasing the sampling frequency of the $P(t)/\Delta T$ curve to 1000 Hz, it is determined that there does not exist any frequency components higher then 0.5 Hz that are of any significance. Therefore, the 1 Hz TDP200 sampling frequency is more than sufficient for its data acquisition. Perfusion effects are examined through simulating the closed form solution to the bioheat equation. It is found that perfusion can cause at least 0.2% variability in K_m, but frequencies around the order of 0.1 Hz can cause up to 2% variability in K_m. On average, perfusion effects force 0.6% variability in mea-

sured value of K_m. Experiments specifically designed for examining perfusion effects are not very conclusive. This is mostly because it is very difficult to design experiments that can specifically address perfusion issues without the interaction of other sources of variability. Probe-tissue contact has always been regarded as a large problem. Experiments designed to address this problem are able to reveal just how serious this problem can be. It is also found that the applied temperature step ΔT plays a role in determining $P_{ss}/\Delta T$ and hence K_m. $P_{ss}/\Delta T$ should only be a function of the medium's thermal conductivity but that is not found to be the case. Experiments done on phantom materials helped determine the dependence of $P_{ss}/\Delta T$ on ΔT. Based on the findings, the impact ΔT plays in causing variability in K_m measurements is quantified. The calibration constants K_b and a are used to take away the K_m dependence on ΔT. There are also speculations that the K_m variability that have been observed might turn out to be due to changes in skin tissue K_m as a result of shifts in the water content of the skin tissue. In this case, the variability observed are not errors but actual K_m changes. This speculation is difficult to verify and even more difficult to quantify. The result of the investigation into the causes of K_m measurement variability are summarized in Table 4.1.

Assuming that each of these variability sources occur independent of one another, the overall percent K_m measurement variability accounted for thus far is equal to the square root of the sum of the squares of percent variability listed in Table 4.1. This value comes out to be about 1.2%. Though this does not totally account for the 1.5% to 2% K_m variability that have been observed, this does account for the majority of it.

The percent variability associated with each of the different sources of variability listed in Table 4.1 are estimates based on either simulations, experimental results, or calculations. These values are only estimates and thus are rough in nature. Neverthe-

less, these values not only give insight into why there exists large variability in skin tissue K_m measurements, but also provide the foundation to solving this problem in the future.

Sources of Variability	% Variability
Precision Limit of TDP200 System	0.2%
Low Sampling Rate of P(t)/ΔT Curve	0.0%
Baseline Fluctuation of Skin Tissue	0.5%
Random Perfusion Effects of the Blood Vessels	0.6%
Non-ideal Probe-Tissue Contact	0.8%
Dependence of K_m on ΔT	0.4%
Changes in Skin Tissue Intrinsic Thermal Conductivity	?%
Total RMS Variability of Quantifiable Sources	1.2%

Table 4.1: Sources of skin tissue intrinsic thermal conductivity variability and their respective contributions

Bibliography

[1] Bowman, H.F., Balasubramaniam, T.A., and Woods, M., "Determination of Tissue Perfusion from 'in-vivo' Thermal Conductivity Measurements," ASME Heat Transfer in Biotechnology, Nov. 1977, 77-WA/HT-40.

[2] Yuan, D. Y., Valvano, J.W., Anderson, G.T., "Measurement of Thermal Conductivity, Thermal Diffusivity, and Perfusion", Biomedical Sciences Instrumentation, Vol. 29, 1993, pp 435-442.

[3] Valvano, Jonathan W., "The Use of Thermal Diffusivity to Quantify Tissue Perfusion", Ph.D. Thesis in Medical Engineering, Harvard-MIT Division of Health Science and Technology, August 1981.

[4] Duck, F. A., Physical Properties of Tissue: A Comprehensive Reference Book, Academic Press, 1990, pp 9-26.

[5] Chato, J.C., "A Method for the Measurement of Thermal Properties of Biologic Materials", Thermal Problems in Biotechnology, New York, American Society of Mechanical Engineers, LCN068-58741, 1968, pp. 16-25.

[6] Balasubramaniam, T.A., "Thermal Conductivity and Thermal Diffusivity of Biomaterials: A Simultaneous Measurement Technique", Ph.D. Thesis, Northeastern University, Boston MA, June 1975.

[7] Holmes, K.R., Chen, M.M., "In-vivo Tissue Thermal Conductivity and Local Blood Perfusion Measured with Heat Pulse-decay Method", The Physiologist, Volume 23, No. 4, August 1980, pp. 183.

[8] Valvano, J.W., Woods, M., Bowman, H.F., "A Microprocessor Based Thermal Diffusion Probe for Blood Flow", Proceedings of the 31st ACEMB, Vol. 20, October 1978.

[9] Bowman, H.F., "Heat Transfer and Thermal Dosimetry," Invited Review Paper, Third International Symposium on Cancer Therapy by Hyperthermia, Drugs and Radiation, Colorado State University, Ft. Collins, Co., June 22-26, 1980, Journal of the National Cancer Institute, Monograph, Vol. 60, 1981.

[10] Valvano, J.W., Allen, J.T., and Bowman, H.F., "The Simultaneous Measurement of Thermal Conductivity, Thermal Diffusivity, and Perfusion in Small Volumes of Tissue," ASME Journal of Biomechanical Engineering, Vol. 106, Aug. 1984, pp.192-197.

[11] Balasubramaniam, T.A., and Bowman, H.F., "Thermal Conductivity and Thermal Diffusivity of Biomaterials: A Simultaneous Measurement Technique," ASME Journal of Biomechanical Engineering, Vol. 99, Aug. 1977, pp. 148-154.

[12] Bowman, H.F., "Estimation of Tissue Blood Flow,", Heat Transfer in Medicine and Biology, Vol. 1. Plenum Publishing Corporation, 1984.

[13] Newman, W.H., Summit, S.C., Balasubramaniam, T.A., Bowman, H.F., "In-vitro and In-vivo Measurements of Low-Level Tissue Blood Flow", Heat Transfer Division of the ASME, Vol. 104, 1988, pp51-56.

Biographical Note

Andy Tsai, born on December 15, 1969 in Taipei, Taiwan, lived in Hsinshu, Taiwan till the age of 11 and immigrated to Alameda, CA on December 27, 1980. His father is a professor of Nuclear Engineering at Tsing Hua University in Hsinshu, Taiwan and his mother owns and operates a sandwich shop in Alameda, CA. He graduated from Alameda High School in 1988.

Andy graduate *summa cum laude* from Revelle College at University of California, San Diego with a B.S. in the field of Electrical Engineering in 1993 while minoring in Economics. He is a founding member of UCSD's chapter of Tau Beta Pi and a member of Phi Beta Kappa. He graduated as co-valedictorian of his class and continued his graduate education at Massachusetts Institute of Technology. He received his M.S. in the field of Electrical Engineering from MIT in May of 1995 and will continue his graduate studies in the Ph.D. program in Medical Engineering and Medical Physics offered by Harvard University - Massachusetts Institute of Technology Division of Health Science and Technology.